Lappeenranta
University of Technology

Irina Turku

ADSORPTIVE REMOVAL OF HARMFUL ORGANIC COMPOUNDS FROM AQUEOUS SOLUTIONS

Thesis for the degree of Doctor of Science (Technology) to be presented
with due permission for public examination and criticism in the Auditorium
of the Student UnionHouse at Lappeenranta University of Technology,
Lappeenranta, Finland on the 21st of December, 2010 at noon.

Acta Universitatis
Lappeenrantaensis 418

Supervisor Adjunct Professor Tuomo Sainio
Department of Chemical Technology
Lappeenranta University of Technology
Finland

Reviewers Professor Ahmet R. Özdural
Chemical Engineering Department
Hacettepe University
Turkey

Professor Rein Munter
Chemical Engineering Department
Tallinn University of Technology
Estonia

Opponent Professor Ahmet R. Özdural
Chemical Engineering Department
Hacettepe University
Turkey

ISBN 978-952-265-027-6

ISBN 978-952-265-028-3 (PDF)

ISSN 1456-4491

Lappeenrannan teknillinen yliopisto

Digipaino 2010

ABSTRACT

Irina Turku

Adsorptive removal of harmful organic compound from aqueous solutions
Lappeenranta 2010
68 p.
Acta Universitatis Lappeenrantaensis 418
Diss. Lappeenrannan teknillinen yliopisto
ISBN 978-952-265-027-6, ISBN 978-952-265-028-3 (PDF), ISSN 1456-4491

Adsorption is one of the most commonly used methods in water treatment processes. It is attractive due to it easy operation and the availability of a wide variety of commercial adsorbents. This doctoral thesis focuses on investigating and explaining the influence of external phase conditions (temperature, pH, ionic strength, acidity, presence of co-solutes) on adsorption phenomena. In order to cover a wide range of factors and phenomena, case studies were chosen from various fields where adsorption is applied. These include the adsorptive removal of surface active agents (used in cleaning chemicals, for example) from aqueous effluents, the removal of hormones (estradiol) from drinking water, and the adsorption of antibiotics onto silica. The latter can be used to predict the diffusion of antibiotics in the aquatic system if they are released into the environment. Also the adsorption of living cells on functionalized polymers to purify infected water streams was studied.

In addition to these examples, the adsorptive separation of harmful compounds from internal water streams within a chemical process was investigated. The model system was removal of fermentation inhibitors from lignocelluloses hydrolyzates. The detoxification of the fermentation broth is an important step in the manufacture of bioethanol from wood, but has not been studied previously in connection with concentrated acid hydrolyzates.

New knowledge on adsorption phenomena was generated for all of the applications investigated. In most cases, the results could be explained by combining classical theories for individual phenomena. As an example, it was demonstrated how liquid phase aggregation could explain abnormal-looking adsorption equilibrium data.

In addition to the fundamental phenomena, also process performance was of interest. This aspect is often neglected in adsorption studies. It was demonstrated that adsorbents should not be selected for a target application based on their adsorption properties only, but regeneration of the spent adsorbent must be considered. It was found that using a suitable amount of organic co-solvent in the regeneration can significantly improve the productivity of the process.

Keywords: adsorption, water treatment, polymeric adsorbent, activated carbon, cationic surfactant, tetracycline, 17 β-estradiol.

UDC 66.081.3: 661.183: 628.16

Preface

First and foremost I would like to thank my supervisor, Adj. Prof. Tuomo Sainio for the guiding me through research. His scientific experience, encouragement, and patience were invaluable to me during these years. I am also deeply grateful to Prof. Erkki Paatero for giving me the chance to start working at his laboratory. I am indebted to reviewers Prof. Ahmet R. Özdural and Prof. Rein Munter for their critical reading and valuable comments on this work.

My sincere thanks go to all my colleagues in the Laboratory of Industrial Chemistry for the creating of the pleasure working atmosphere during all these years. I also would like to thank all my friends in Finland and Russia. Especial thanks to Dr. Sergei Preis for the important comments to my work and the language revising. Thanks also to Dr. Svetlana Butylina for interesting and educative discussions. My deep gratitude goes to St. Petersburg to my friend Elena Levykina, whose support and encouragement were very important for me.

Special thanks for the personal grant from the Research Foundation of Lappeenranta University of Technology.

Finally, my warmest thanks to my closest people, to my family, whose love, support, and understanding were invaluable through this study.

Lappeenrata, December 2010

Irina Turku

LIST OF PUBLICATIONS

I **Turku, I.**, Sainio, T., Thermodynamics of tetracycline adsorption on silica, *Environment Chemistry Letters*, 5 (2007) 225–228.

II **Turku, I.**, Sainio, T., Modeling of adsorptive removal of benzalkonium chloride from water with polymeric adsorbent, *Separation and Purification Technology*, 69 (2009) 185–194.

III **Turku, I.**, Sainio, T., Paatero, E., Adsorption of 17β-estradiol onto two polymeric adsorbents and activated carbon, Proceedings of ICheaP9 conference, 10-13.5.2009, Rome, Italy, Published in *Chem. Eng. Trans*., 17 (2009), 1555–1560.

IV Sainio, T., **Turku, I.**, Adsorption of cationic surfactants on a neutral polymeric adsorbent: Investigation of the interactions by using mathematical modeling, *Colloids and Surfaces A: Physicochemical and Engineering Aspects*, 358 (2010) 57–67.

V Sainio, T., **Turku, I.**, Heinonen, J., Adsorptive removal of fermentation inhibitors from concentrated acid hydrolyzates of lignocellulosic biomass, submitted to Bioresource Technology in October 2010.

The author's contribution in the publications

I The author planned and carried out all experiments and analyzed data. The paper was written together with the co-author.

II The author carried out all experiments and analyzed data. The paper was written together with the co-author. The author did not participate in the model development.

III The author planned and performed the experiments, analyzed data and prepared the manuscript.

IV As in publication **II**.

V The author planned and carried out most of the experiments. Data was analyzed and the manuscript prepared together with the co-authors.

TABLE OF CONTENTS

NOMENCLATURE

Symbols

A	surface area	mm^2
A	Hamaker constant	J
b	Langmuir coefficient	L/g, L/mol
c^L	liquid phase concentration	mol/L
d	separation distance	nm
e	elementary charge	C
q_s	adsorption capacity	mol/L, g/L
q, Q	solid phase concentration	mol/L, g/L
I	ionic strength	mol/L
k_B	Boltzman constant	J/K
V^L	liquid phase volume	L
m	mass of adsorbent	g
n	aggregation number	-
N_A	Avogadro constant	mol^{-1}
R_p	particle radius	m
T	absolute temperature	K
ε_0	permittivity of vacuum	F/m
ε_r	permittivity of water	F/m
ε_p	porosity of adsorbent	-
ζ	zeta potential	mV
κ	Debye-Hückel parameter	nm
λ	correlation length of molecule in liquid	Å
ρ	density of adsorbent	$g\ L^{-1}$
$\Delta_{ads}H$	enthalpy of adsorption	$kJ\ mol^{-1}$
$\Delta_{ads}G$	Gibbs energy of adsorption	$kJ\ mol^{-1}$
G^{AB}	acid-base interaction energy	kT

G^{EL}	electrostatic interaction energy	kT
G^{LW}	Lefshitz-van der Waals interaction energy	kT
$\Delta_{ads}S$	entropy of adsorption	kJ mol^{-1} K^{-1}

Abbreviations

BV	Bed volume
DLVO	Derjaguin-Landau-Verwey-Overbeek
EDC	Endocrine Disruptor Compounds
HPLC	High Performance Liquid Chromatography
IEP	Isoelectric point
SCF	Self-consistent field
UV-VIS	Ultraviolet-Visible

1 INTRODUCTION

1.1 ADSORPTION PHENOMENON

1.1.1 Types of adsorption

Adsorption is defined as a phenomenon during which the concentration of solute increases at the surface or the interface between two phases. This definition includes chemisorption, physical sorption and ion-exchange. An *adsorbate* is a chemical substance transferred from the liquid phase to the solid one during adsorption. An *adsorbent* is a solid phase accumulating the adsorbate. Gas-solid or gas-liquid adsorption was not considered here.

The driving forces of the adsorption process have been widely discussed in earlier studies and are usually considered as follows [1]:

- Ion-exchange: replacement of counter ions of the double layer by similarly charged solute ions
- Ion pairing: electrostatic interactions between counter ions
- Acid-base interaction: hydrogen-bond formation between adsorbent and solute
- Adsorption by polarization of π-electrons: interaction between aromatic molecule groups and positive charges at the adsorbent surface
- Adsorption by dispersive forces
- Hydrophobic bonding: attractive interaction between hydrophobic groups of solute molecules and the adsorbent surface

The given interaction forces differ in their energy of bonding, as shown in Table 1.

Dependent on the forces involved in adsorption, its mechanisms can be divided into two fundamental types*: physical sorption* and *chemisorption* [2]. The general features which distinguish physical adsorption and chemisorption are given in Table 2 [2].

Table 1 Molecule - molecule interaction energies [1].

Interaction parameters	Interaction energy (kJ/mol)
Covalent or chemical bonding forces	200–800
Charge–charge	600–1000
Interaction between polar molecules	< 40
Dispersion forces	~ 1
Hydrogen bonding	10–40
Hydrophobic interaction	< 20
Hydrophilic interaction	< 20

Table 2 General properties of physical and chemical sorption [2].

Physical sorption	Chemisorption
• Low heat of adsorption • Non specific • Monolayer or multilayer • No dissociation of adsorbed species • Rapid, reversible • No electron transfer, although polarization of sorbate may occur	• High heat of adsorption • Highly specific • Monolayer only • May involve dissociation • May be slow and irreversible • Electron transfer leading to the bond formation between sorbate and surface

Physical sorption involves relatively weak intermolecular forces, such as van der Waals forces, hydrogen bonding, and hydrophobic interactions. This is non-specific weak interaction between adsorbed molecules and a solid surface. In this interaction, the adsorbed molecules are not fixed to the specific site of the adsorbent and can move over

the surface. In chemisorption, molecules adhere to the surface due to formation of chemical, usually covalent, bonds between adsorbed molecules and a solid surface.

The main difference between physical and chemical sorptions is the magnitude of enthalpy of the adsorption. The enthalpy values smaller than 20 kJ/mol correspond to physical sorption, while the values higher than 80 kJ/mol correspond to chemisorption [1, 3, 4].

The adsorption of solute on solid/liquid interface depends on many factors, such as:

- physico-chemical properties of the solid surface (porosity, surface area, presence or absence of charged or non-polar groups);
- the nature of the solute (pK_a, hydrophobicity, molecular size);
- properties of the liquid phase (pH, salt concentration, temperature, presence of the competitive solute);
- complexation in the liquid phase.

1.1.2 Adsorbent materials in water treatment processes

Adsorption is a commonly used method in water treatment and other separation processes. Among the other methods, adsorption is fast and simple in operation. The key factor for the adsorption process is the choice of adsorbent. A good quality adsorbent should have fast kinetics of interaction with the adsorbate, porous structure resulting in high surface area and high adsorption capacity. Another important aspect in adsorptive water treatment processes is the regeneration of spent adsorbent.

Activated carbon and silica gel were used as adsorbents at earlier stages of the water adsorptive treatment. With the increasing economical demands, the new adsorbents, such

as zeolites and ion-exchange resins, for practical separation processes were applied and developed.

Activated carbon, the most common adsorbent for water treatment [5], is prepared from carbonaceous materials, such as wood, peat, coals, coconut shell, petroleum coke, and bones, using *gas* or *chemical activation* methods. The gas activation first involves carbonization at 400-500 °C to eliminate the bulk and the volatile matter, and then partial gasification at 800–1000 °C to develop the porosity and surface area. The chemical method involves impregnation of row material with chemicals such as H_3PO_4, KOH, or NaOH after that carbonization at temperature between 500 to 900 °C [6]. Activated carbon is available in two main forms: powdered activated carbon (PAC) and granular activated carbon (GAC). GAC is more practical being simple in operation and separation from the liquid phase. On the other hand, PAC requires shorter contact times in operation. Activated carbon is preferred to other adsorbents in wastewater treatment because of its non-selectivity, i.e. ability to adsorb various types of pollutants including phenols, dyes, pesticides, detergents, and metals [7]. However, activated carbons cannot be considered as low-cost adsorbents. For example, in the purification of industrial and domestic wastewaters, the share of the activated carbon adsorption comprises approximately 26% of the total treatment cost [8]. The main disadvantage of activated carbon, however, is economically unfeasible regeneration after the loading cycle [9, 10]. Treatment at high temperatures is the most common regeneration method for exhausted activated carbons. The thermal regeneration process has high energy requirements and, therefore, is expensive. Moreover, the adsorbent is lost at high temperatures due to its decomposing, thereby making the regenerated product of a lower capacity than the parent product. Also, the regeneration of activated carbon is often carried out at installations belonging to the manufacturer or distributor of the activated carbon, creating logistic and safety problems. Besides thermal regeneration, several solvent regeneration techniques, such as acetone [11], NaOH [12], and peroxide [13] are known.

Silica gel is prepared by the coagulation of colloidal silicic acid [6]. Under suitable pH conditions, silicic acid, $Si(OH)_4$, has a tendency to polymerize and form a network of siloxane (Si-O-Si). At the same time, some of the Si-O-H groups remain free and become functional groups. Silica gel as an adsorbent is used in many industries as a desiccant and purifying agent [7, 14]. After the drying procedure, silica is easily regenerated at 150 °C.

Zeolites are inorganic adsorbents that occur naturally and are also prepared synthetically as crystalline aluminosilicates of alkali or alkali earth elements. They are used as an ion-exchange selective adsorbent [15] as well as a molecular adsorbent [16, 17, 18, 19]. The thermal regeneration method of zeolites is not feasible due to its high energy cost and decreased adsorption capacity compared to the parent adsorbent [20]. The use of the Fenton oxidation method also reduced the adsorption capacity [19]. Using 99% ethanol for the regeneration of zeolite was effective but not environmentally friendly due to the potential ignition of ethanol at high concentrations [16].

In recent years, different polymeric adsorbents, such as ion-exchange and nonionic resins were considered as an alternative to activated carbon for the selective removal of organic pollutants from aqueous solutions [9, 20-26]. The majority of nonionic polymeric resins are based on the cross-linked polysterene or acrylic matrix. After the polymerization, the required active groups can be introduced into the matrix, after which the resins are used as adsorbents through a cation or anion exchange mechanism. Cationic exchange resins generally contain bound sulfuric acid groups, carboxylic, phosphoric, or arsenic groups. Anionic resins generally contain strongly basic quaternary amino groups or other weakly basic amino groups [27]. Typically, adsorption onto polymeric adsorbents is exothermic reaction with low enthalpy, which suggests physical sorption or transitional sorption between chemical and physical ones [21, 22]. Due to the physical nature of the adsorption forces, the regeneration of the adsorbent can easily be accomplished with bases and organic solvents [9, 21-26].

For large scale operation in industrial processes, a large amount of adsorbent is usually needed. This makes its cost one of the competitive parameters. In Table 3 the costs of adsorbents are taken from the price lists of delivery company [28]: one can see that

polymeric adsorbents are the most expensive and activated carbon and silica gel range at approximately a similar cost level.

1.1.3 **Adsorption process unit operation**

Fixed bed adsorption is mostly used for the large scale operations, such as water treatment and other separation processes. In Fig. 1A the fixed bed operation is schematically shown. In a packed bed, the adsorbent particles comprise the stationary phase, and liquid is pumped through the adsorbent bed. Dynamic adsorption occurs across mass transfer zones (equilibrium stages) which progress down the adsorbent bed. Thus, the number of equilibrium stages is maximized giving a good result for the adsorption/separation. The main characteristic of the fixed-bed reactor work is the *breakthrough curve*, which presents the outlet concentration of the adsorbate as a function of time or treated volume (Fig. 1B). In Fig. 1 C/C_0 is the outlet relative concentration versus the volume of treated effluent. The outlet concentration, at which the operation should be stopped from meeting the treatment target, is called *the break point.*

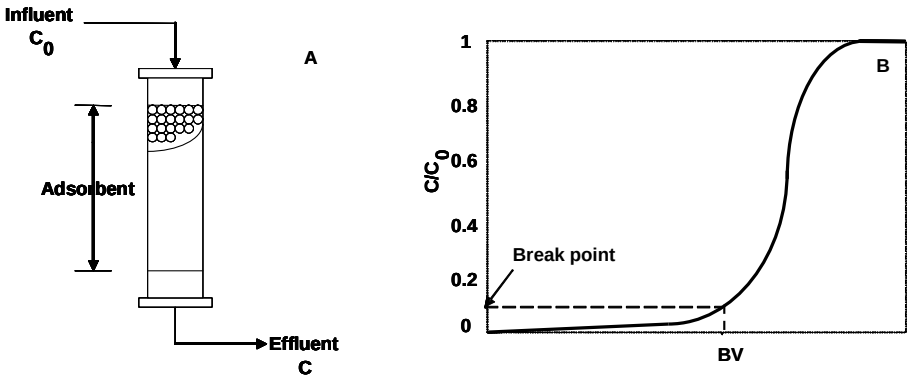

Figure 1. (A) Fixed bed operation; (B) Breakthrough curve.

Breakthrough curves always have an S shape with variations in their steepness and the position of the break point. The effectiveness of a fixed bed operation is influenced mainly by equilibrium (adsorbent capacity) and the adsorption kinetics of the solute

(diffusion and dispersion coefficients of solute) [2, 29]. In addition, the depth of the column of the adsorbent and the velocity of the flow are factors which influence the shape of the breakthrough curve. Adsorption equilibrium is quantitatively described by the *adsorption equilibrium isotherm*, which is the dependence of the amount of solute adsorbed per unit of the solid phase mass (surface area, volume) on the equilibrium solution concentration. The adsorption isotherm is useful for describing the adsorbent capacity for a given solute. There are many types of isotherms known for various solutes and adsorbents [2]. The shape of the isotherm depends on the adsorbents' and adsorbates' nature, and the parameters of solution (pH, salinity, temperature). The adsorption isotherms are basically related to equilibrium conditions. However, the time for achieving the equilibrium is also important for the determination of feasibility of the treatment process. The structure of adsorbents is usually porous giving a developed surface area. This makes the pore diffusion rate a highly important limiting kinetic factor. Thus, the time spent for achieving the adsorption equilibrium should be as short as possible. Therefore, the proper adsorbent should have an optimum trade-off between the high adsorption capacity determined by its developed porous structure and the adsorption kinetics to achieve the equilibrium in a sensible time.

1.2 OBJECTIVES AND STRUCTURE OF THE WORK

The research objectives include the disclosure of adsorption regularities for the aqueous pollutants of high environmental hazard priority, pharmaceuticals, and fermentation inhibitors at the adsorbents of interest. The adsorption type, i.e. kinetics and thermodynamics of adsorption, for polymeric adsorbents, activated carbon and silica gel had to be established by means of generally applied research methods - establishing the time-dependent curves of adsorption, and the adsorption equilibrium curves dependent on the impact factors, pH, temperature, solution ionic strength, and the content of organic solvents. As a result of these studies, the operation parameters of the adsorptive treatment

of aqueous solutions were targeted. The study includes a comparison of the adsorbents in order to optimize the separation of target solutes in both batch and fixed-bed experiments.

Papers I to IV present the results on the impact of various factors, such as ionic strength, pH, temperature, presence of a co-solvent, and aggregation of solutes on adsorption. Papers II and V also consider the performance of adsorption processes in removing the target component(s) from aqueous solutions.

The summary also includes some previously unpublished data on the adsorption of living microorganisms on solid adsorbents.

2 MATERIALS AND EXPERIMENTAL METHODS

Materials

Five polymeric adsorbents were used: Amberlite XAD–16 (styrenic matrix, nonionic), Amberlite XAD–7 (acrylic matrix, nonionic), CS16GC (styrenic matrix, strong acid cation–exchanger, sulfonated, H^+–form), Dowex 66 (styrenic, weak basic anion-exchanger, Cl^-–form), Purolite A835 (acrylic, weak basic anion-exchanger, Cl^-–form), an activated carbon and a silica gel. The properties of the adsorbents are presented in Table 3.

In Figs. 2 and 3 present the chemical structures of solutes which were used for the adsorption experiments. Fig. 2 presents the pollutants studied in Papers I to IV. The hormone 17β-estradiol (Fig. 2A) is an estrogenic female hormone, produced by human glands and excreted in the urine and feces. Also, the natural and synthetic estrogens are used as oral contraceptives, and up to 80% is excreted as unmetabolized conjugates [30]. Antibiotic tetracycline (Fig. 2B) is used to treat both human and animal infections. It is suggested that 90% of the administered dose of antibiotics may be excreted through the urine and feces [31]. Benzalkonium chloride (BKC) (Fig. 2C), the cationic surfactant, is

used as biocide in medicine. Cationic surfactants are not biodegradable under anaerobic conditions, and degrade only slowly under aerobic conditions [32, 33].

The presence of the residuals of medical drugs in surface, ground and drinking water was reported in many countries [32, 34-36]. The different studies suggest that the presence of certain pharmaceuticals in the environment cause ecological hazards. Jørgensen and Halling-Sørensen have classified possible effects into three groups [33]. The presence of antibiotics in the soil, and ground and surface waters caused a genetic selection of more resistant bacteria, shifting the equilibrium in the microbial community in the ecosystem. Also, the presence of an antibacterial agent in the environment in low concentrations has allowed bacterial flora to develop a resistance to those agents [33, 34]. Hormone 17β-estradiol belongs to the endocrine disrupter compounds (EDC) group, i.e., chemicals which can disturb the normal function of the endocrine system of a living organism [35]. They have a harmful effect on the normal development of the reproductive tract and also the immune system. The observed impacts of EDCs on wildlife include the feminization of fish, and masculinization and reproductive abnormalities in birds and turtles. For the human, they can permanently alter the reproductive tract and physiology, increasing the risk of cancer [30, 36-42].

Fig. 3 presents the adsorbates studied in Paper V. These compounds are formed during the acid hydrolysis of cellulose material [43, 44]. Furfural, hydroxymethylfufural, and acetic acid (Fig. 3) are the inhibitors of the bioconversion of glucose into ethanol [45-47].

Table 3. Properties of adsorbents according to product sheet.

Type of adsorbent	Parameter	Values
Amberlite XAD-7	Surface area	450 m^2 /g
	Average pore diameter	90 Å
	Wet mesh size	20-60
	True wet density	1050 g/L
	Price	5.600–10.000 $/$m^3$
Amberlite XAD-16	Surface area	800 m^2 /g
	Average pore diameter	100 Å
	Wet mesh size	20-60
	True wet density	1020 g/L
Finex CS16GC	Surface area	-
	Average pore diameter	gel type
	Wet mesh size	-
	True wet density	1190 g/L
	Price	5.600–10.000 $/$m^3$
Dowex 66	Surface area	10.24 m^2 /kg
	Average pore diameter	macroporous
	Wet mesh size	-
	True wet density	1065 g/L
	Price	5.600–10.000 $/$m^3$
Purolite A835	Surface area	6.36 m^2 /kg
	Average pore diameter	macroporous
	Wet mesh size	-
	True wet density	1072 g/L
	Price	5.600–10.000 $/$m^3$
Activated carbon	Surface area	-
	Average pore diameter	-
	Wet mesh size	-
	True wet density	1350 g/L
	Price	500–1.800 $/t
Silica gel	Surface area	700 m^2/g
	Average pore diameter	mesoporous
	Wet mesh size	-
	True wet density	-
	Price	500–1.100 $/t

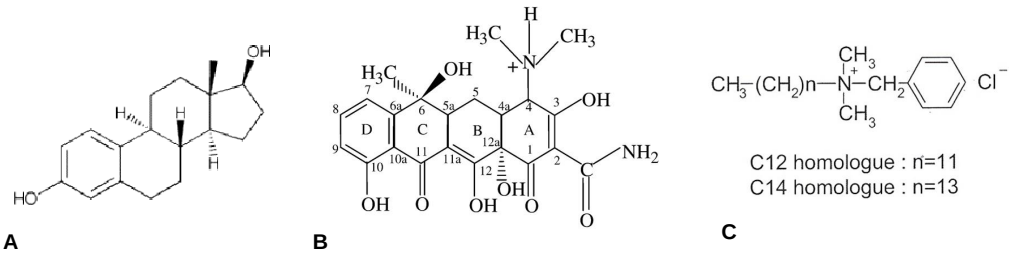

Figure 2. Chemical structure models of (A) 17*β*-estradiol, (B) tetracycline molecules, and (C) BKC homologues, benzyldimethyldodecyl ammonium chloride (C_{12}) and benzyldimethyltetradecyl ammonium chloride (C_{14}).

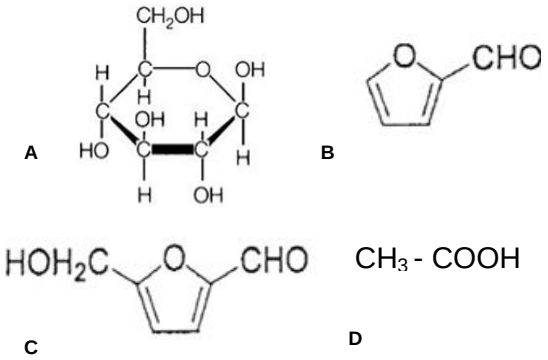

Figure 3. Chemical structure models of (A) glucose, (B) furfural, (C) hydrohymetylfurfural, and (D) acetic acid.

Methods

Equilibrium and kinetic measurements in batch system

Adsorption equilibrium and adsorption kinetics experiments were carried out in the batch system with the appropriate amount of solid adsorbent placed into the flask with solute diluted in the aqueous phase with a known concentration. An orbital shaker with thermoregulation was used for the mixing and keeping the temperature constant.

The adsorption kinetics experimental data were used for the determination of the intraparticle diffusion coefficients (Paper II) as well as for the determination of the solute concentration equilibrium between the liquid and solid phases. The experiments were conducted at a sufficiently high rotation rate in order to eliminate a liquid mass transfer resistance.

Changes in the liquid phase concentration were monitored by periodical sampling from the batch adsorber. The samples were returned to the flask in order not to change the phases ratio. The adsorption kinetics of surfactants was slow, making the acquisition of the kinetic data sufficiently accurate. The adsorption kinetics for furfural, hydroxymethylfurfural, glucose, and acetic acid was fast thus making attempts to measure the initial adsorption kinetics ineffective.

In the experiments with 17 β-estradiol and tetracycline the flasks were covered by tinfoil to prevent the possible photodegradation of the solute.

Column dynamics experiment

The dsorption and desorption of surfactants and acid hydrolyzation products were studied in glass columns of 1.5 to 1.6 cm in inner diameter. The void fraction (ε_p) of the packed column (*i.e.* porosity), was estimated from the retention volume of the NaCl (for XAD-16 and activated carbon) or HCl (for cation-exchanger CS16GC) solution. The amount of 0.1 mL of 0.5 M NaCl or HCl was injected as a pulse and eluted with Millipore water at

the flow rate of 0.05 mL/min. The outlet signal was monitored with an online conductivity detector. The void volume of the packed column was calculated from the equation:

$$V_{\underset{\text{volume}}{\text{void}}} = V_{\text{NaCl or HCl ret}} - V_{\text{tube}} - \frac{1}{2}V_{\text{injection}} \ , \qquad (1)$$

where $V_{\underset{volume}{void}}$ is the column void volume, $V_{\text{NaCl or HCl ret}}$ is the retention volume of NaCl or HCl, V_{tube} is the volume of the tubings in the system, $V_{\text{injection}}$ is the injection volume of the NaCl solution.

The void volume of the tubing system was determined by the injection of Blue Dextran (1.5 g/L).

The aqueous solution of the solute was fed into the column at a constant flow rate by using a pump. The outlet concentration of the surfactant was monitored online by a spectrophotometer. The outlet concentrations of glucose and inhibitors were collected and measured with HPLC (see Papers III and V).

Solutes concentration measurements

The liquid phase concentration of surfactants and tetracycline was measured by using a UV/VIS spectrophotometer. Concentrations of glucose, furfural, hydroxymethylfufrural, acetic acid, and estradiol were measured by using HPLC equipment.

Critical micelle concentration measurement

The critical micelle concentrations of surfactants as well as surfactants mixtures were measured by using a KSV Sigma 700/701 tensiometer.

‘

Measurement of zeta potential

The zeta potentials of the bacteria, resins, and activated carbon were measured by using Coulter Delsa 440. The samples were resuspended in the solution and diluted to an optical density of 0.4-0.6. The zeta potentials of the resins and activated carbon were measured from samples powdered with a mortar. All measurements were repeated three or four times, and average values were reported.

Contact angle measurements

For the determination of interaction energies between bacteria cells the contact angles meter CAM 100 was used. The contact angles of water, formamide, and diiodomethane on the bacteria surface were measured by the sessile drop technique on a $2 \cdot 10^8$ cells/mm bacterial layer. The bacterial lawns were obtained by the filtering cell suspension through a membrane filter with a 0.45 μm pore size (Schleicher & Schüll) with the backpressure technique.

Bacterial cells counting

The bacterial population was determined by using the calibration curve of *turbidity* vs. the number of viable bacteria. The number of viable bacterial cells was determined by the serial dilution plate count. The amount of 0.5 ml from the bacterial suspension was serially diluted by the factor 1:10 in test tubes containing 4.5 ml of 9% NaCl for a total of 6-8 times. In total, 0.1 ml from dilution test tubes was spread onto Petri dishes. The Petri dishes were incubated at 37 °C for 24 hours, and subsequently, the growth colonies were counted. The turbidity of the bacterial suspension was measured by using a UV-VIS spectrophotometer at a 600 nm wavelength.

Polymeric adsorbent particle size determination

The particle size distribution was obtained for a water-swollen polymer by photographing with an optical microscope.

The effective particle radius, R_p, was calculated with the equation

$$R_p = \frac{3V_{sample}^{tot}}{A_{sample}^{tot}}, \quad (2)$$

where V_{sample}^{tot} is the total volume of the sample, mm^3 and A_{sample}^{tot} is the total surface area of the sample, mm^2.

Estimation of thermodynamic parameters

The standard thermodynamic functions, the thermodynamic equilibrium constant, K, Gibbs energy changes, $\Delta_{ads}G$, enthalpy changes, $\Delta_{ads}H$, and entropy changes, $\Delta_{ads}S$, can be determined from the slope of the adsorption isotherm.

The thermodynamic equilibrium constant, K, the ratio of the activities of the component in the liquid and solid phases, is the initial slope of the adsorption isotherm and it can be estimated by

$$K = \lim_{c \to 0}(q/c) = qb, \quad (3)$$

where q is the maximum adsorbed amount and b the equilibrium constant.

The equilibrium constant is related to the Gibbs energy, $\Delta_{ads}G$, by the equation

$$\Delta_{ads}G = -RT \ln K. \quad (4)$$

The enthalpy, $\Delta_{ads}H$, and entropy, $\Delta_{ads}S$, can be obtained from the Eq. 5:

$$\Delta_{ads}G = \Delta_{ads}H - T\Delta_{ads}S. \quad (5)$$

Substituting Eq. (4) into (5), gives

$$-RT \ln K = \Delta_{ads}H - T\Delta_{ads}S. \quad (6)$$

The division of both sites of Eq.6 by ($-RT$) results in the relation

$$\ln K = -\frac{\Delta_{ads} H}{RT} + \frac{\Delta_{ads} S}{R}. \quad (7)$$

A plot ln$K$ versus 1/T yields $-\Delta_{ads}H/R$ from the slope and $\Delta_{ads}S/R$ from the intercept.

In addition, $\Delta_{ads}H$ can be derived form the van't Hoff equation:

$$\frac{d \ln K}{dT} = \frac{\Delta_{ads} H}{RT^2}, \quad (8)$$

which can be integrated to give

$$\ln\left(\frac{K}{K_{ref}}\right) = \frac{-\Delta_{ads} H}{R}\left(\frac{1}{T} - \frac{1}{T_{ref}}\right). \quad (9)$$

Here, K_{ref} is the equilibrium constant (at infinite dilution) at a reference temperature T_{ref}.

3 RESULTS AND DISCUSSION

3.1 INFLUENCE OF THE LIQUID PHASE PROPERTIES ON ADSORPTION

The factors affecting the adsorption equilibrium include the solution pH, salt concentration, and temperature as well as the presence of organic solvents (polarity of the solution). In this part analyzes the influence of those parameter on the examples of different systems, including also the experimental data of the adsorption of bacteria onto ion-exchange resin. These data have not been published, but describe the phenomenon relevant to this work.

3.1.1 **Effect of pH on adsorption**

The pH of the solution has a complex effect on the process adsorption involving the electrostatic interaction, since the pH can affect the electrical properties of the solid surface as well as the solute.

The electric charge of the substance is characterized by *zeta potential*, which depends on the number of protonated/unprotonated functional groups. The pH at which a substance has equal numbers of negatively and positively charged sites is called the *isoelectric point* (IEP). At pH values lower than the IEP, the net surface charge is positive and anion adsorption is dominant whereas at pH values higher than the IEP the net charge is negative and cation adsorption occurs.

Some substances may consist of a combination of non-polar and ionizable functional groups. The degree of deprotonated groups can be estimated using the Henderson-Hasselbalch equation [48]:

$$[A^-]/[HA]=10^{(pH-pKa)} \quad . \qquad (10)$$

where pKa is the dissociation constant of the corresponding group.

17 *β-estradiol*

Fig. 4 shows the equilibrium adsorption result of estradiol on two nonionic polymeric adsorbents, XAD-16 and XAD-7, and activated carbon.

The functional group of estradiol molecule is hydroxyl group at the first aromatic ring with pKa value equal to 10.4 [30]. It means that at a pH greater than 10.4, the amount of deprotonated hydroxyl groups is larger than that of the protonated ones. Thus, negatively charged ionic estradiol will dominate, whereas at a pH less than 10.4, estradiol molecules are mostly in non-ionic form. According to zeta potential measurements, activated carbon has an IEP at pH 4 (Fig. 5). According to the results in Fig. 4C, the adsorption decreases to its minimum at pH = 10, which is the result of repulsive electrostatic interaction between uniformly charged estradiol molecules and an activated carbon surface.

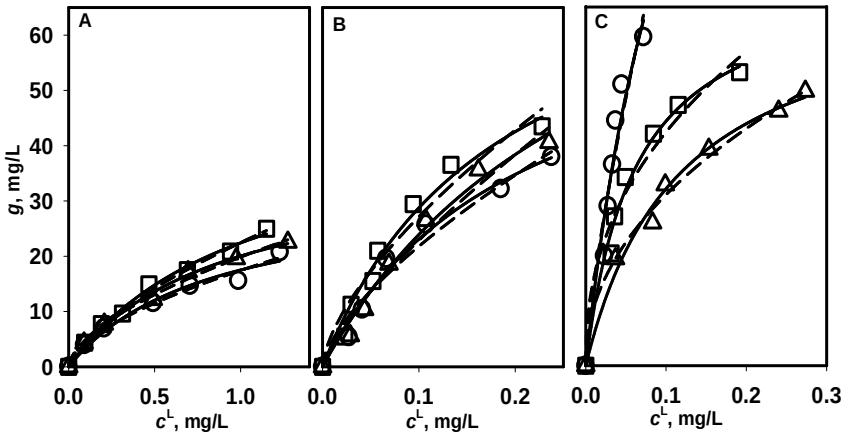

Figure 4. Adsorption of 17 *β*-estradiol on (A) XAD-7, (B) XAD-16, and (C) AC at different pH: (○) 4, (□) 6, (Δ) 10.

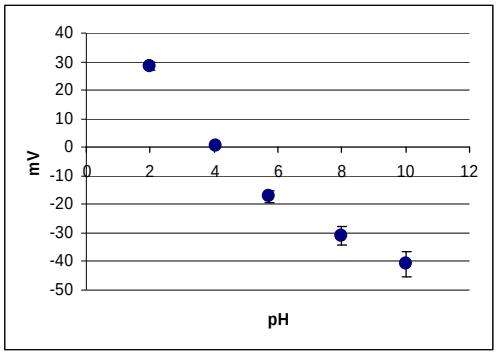

Figure 5. Zeta potential of activated carbon *vs*. pH.

During the adsorption of estradiol on polymeric adsorbents, it was found that pH had a small effect on the adsorption (Figs. 4A and 4B). Unlike activated carbon, the polymeric adsorbents have no functional groups on their surfaces, which can be affected by the pH. Estradiol molecules adsorb mainly due to the hydrophobic nature of the adsorbent and the molecules themselves. The hydrophilic XAD-7 adsorbent had a minimal adsorptive capacity.

The finding meets the support of the other researchers' report: the comparison of adsorption of estradiol onto hydrophilic silica and alumina, and hydrophobic polymeric adsorbents showed the predominant effect of hydrophobic interaction in adsorption. The adsorption of the neutral molecules of estradiol on nonionic polymeric adsorbent was a lot superior to the one at slilica and alumina [49].

Tetracycline

The pH was important parameter in the adsorption of the tetracycline onto silica gel. The tetracycline molecule has multiple functional groups and can be both protonated and deprotonated at a given pH. As a result, these compounds can have cationic, anionic, and neutral or zwitteronic forms as a function of the pH. Tetracycline molecule contains three ionizable groups, tricarbonyl, dimethylammonium, and phenolic β-diketone, the pKa

values of which are 3.3, 7.7, and 9.7, respectively [50]. The total charge of the tetracycline molecules *vs*. pH, calculated by using the Henderson-Hasselbach relationship, is presented in Fig. 6.

The silica surface has a functional group and, therefore, the pH plays an important role in the surface charge generation. The functional groups of silica are silanol groups and the surface charge of the silica is determined by relative concentration of their protonated and deprotonated forms:

$$SiOH + H^+ \leftrightarrow SiOH_2^+ \quad (11)$$

$$SiOH + OH^- \leftrightarrow SiO^- + H_2O \quad (12)$$

The IEP of silica is reported to be at approximately pH 2. The density of negative charges remains low below pH 6, and increases sharply between pH 6 and 11 [51]. For the investigation of the pH influence on the tetracycline uptake by silica, adsorption experiments were conducted at pH 4, 6, and 8. The results are shown in Fig. 7 and indicate that the adsorption amount decreased with the increasing pH. This result can be attributed to the changing of the protonated silanol group concentration on the silica surface. The maximum adsorption was at pH 4, at which silanol groups are protonated. At the same pH tetracycline is in the protonated and zwitzeronic forms. It means that the adsorption mechanism includes mainly the formation of hydrogen bonds between protonated silanol groups and keto-groups of tetracycline molecule. In the transition from acidic to neutral and alkaline conditions, the molecules of tetracycline change from zwitzeronic to anionic [50], and on the surface of the silica the concentration of deprotonated silanol groups increases, inducing the negative charge (Fig. 6). Thus, the decreasing of the adsorption at pH 6 and 8 was due to electrostatic repulsion between uniformly charged surfaces.

The similar results of the tetracycline molecules onto silica were described by Slishek et al. [52]. Also, pH largely effects onto adsorbed amount of tetracycline onto the clay

particles. The adsorption was high at low pH where electrostatic attraction between the negatively charged clay particles and positively charged tetracycline molecules was main factor. At the high pH, hydrogen bonding and hydrophobic interaction were driving forces of the adsorption [53]. The hydrophobic interaction was predominant driving forces of the adsorption onto nonionic polymeric adsorbents [48]. Study the adsorption of antibiotic tetracycline onto aromatic and aliphatic ester polymeric adsorbents shown that tetracycline had higher affinity to aromatic adsorbent.

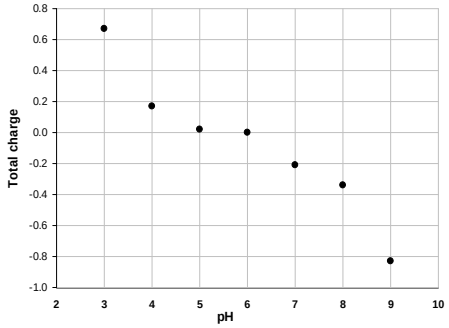

Figure 6. Theoretically calculated total charge of the tetracycline molecule *vs*. pH.

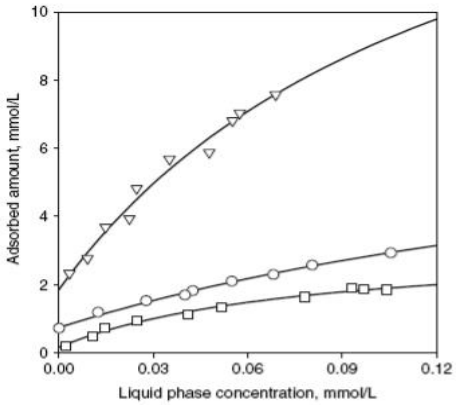

Figure 7. Effect of external solution pH on adsorption of tetracycline on silica (T = 296 K, I = 0.1 mmol/L). Symbols: experimental data at pH = 4 (inverted triangle), pH = 6 (open circle), and pH = 8 (open square).

3.1.2 **Influence of ionic strength on the adsorption**

As it was mentioned above, the ionic strength of the liquid phase is factor which can influence on the adsorption. Mostly, the influence of the ionic strength on the adsorption is related to the decreased thickness of the "electrical double layer" of the charged surface or/and to the "salting out" effect.

Electrical double layer

The solid surfaces have either a positive or a negative charge in the aqueous medium due to the presence of charged functional groups on the surface. Any charged surface immersed in the liquid must be neutralized by oppositely charged ions. Oppositely charged ions arrange near the surface and create a so-called '*electrical double layer'*. Since the overall charge must be neutral, the net charge on one side of the interface must be balanced by an equal net charge of the opposite sign on the other side of the interface.

The main characteristic of the electrical double layer is its thickness, 1/κ, called the Debye-Hückel length given by the expression

$$1/\kappa = \sqrt{\frac{\varepsilon_0 \varepsilon_r k_B T}{2 \times 10^3 e^2 N_A I}}, \qquad (13)$$

where κ is referred to as the Debye-Hückel parameter. The inverse κ is the Debye-Hückel screening length called the double-layer thickness, ε_0 and ε_r are the permittivity of vacuum and the relative permittivity of water, k_B is the Boltzman constant, T is the absolute temperature, e is the elementary charge, N_A is the Avogadro constant, I is the ionic strength of the surrounded media.

With the increasing of ionic strength, the double layer thickness decreases resulting in a decreasing surface charge.

"Salting out" effect

The decrease of the solubility of a component due to the presence of electrolyte is related to the "salting out" effect [54]. It is because of high the concentration of electrolyte removing water molecules from hydrated solute molecules.

In the frame of this work, the influence of the electrolyte on the adsorption was investigated in different systems.

17 *β-estradiol*

Experiments showed that the presence of electrolyte promotes the adsorption of estradiol onto activated carbon (Fig. 8C). At the pH applied in the experiments (pH=6), the activated carbon was negatively charged (Fig. 5). Molecules of estradiol (pKa=10.4) are uncharged in these conditions. Since the double layer thickness at the adsorbent surface is reciprocal to the ionic strength of the solution, the influence of the electric charges at the carbon surface decays with the increasing salt concentration. As a result, the neutral estradiol molecules are adsorbed more strongly onto the less charged surface of AC. Another possible explanation can be related to the decrease of aqueous solubility due to the presence of salt (salting out effect). As a result, the estradiol molecules may form aggregates in the liquid phase and at the surface of adsorbent particles [56]. The similar effect, decreasing of estradiol adsorption onto activated carbon particles with the increase salt concentration was observed by Zhang and Zhou [57].

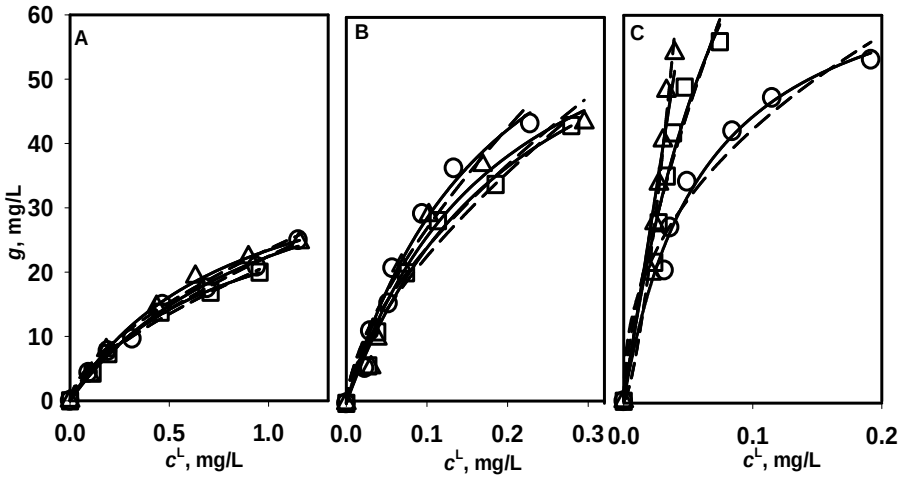

Figure 8. Effect of external solution ionic strength on estradiol adsorption on: (A) XAD-7, (B) XAD-16, (C) AC. Symbols: experimental data at 0.1 mM (○), 20 mM (□), and 100 mM (Δ). Lines: solid line – Langmuir model, dashed line – Freundlich model.

Tetracycline

The presence of electrolytes reduced the adsorption of tetracycline on the silica gel surface; the results are shown in Fig. 9. In the pH range used in the experiments, both the adsorbate and the adsorbent were uniformly charged. The increase of ionic strength reduces the double layer thickness, and thereby, the electrostatic repulsion between the adsorbent surface and the adsorbate molecules decreases, which should result in improved adsorption. Nevertheless, the adsorption of tetracycline decreases with the increasing electrolyte concentration. The explanation of this phenomenon consists of the crucial role of the small pore size of silica particles.

As it is well known, silica is a strongly hydrated solid. However, in the presence of electrolyte, the reduced hydration forces may result in the dehydration of the silica surface. This may consequently reduce the swelling of the silica [58], thus reducing the

pore size of the silica, and subsequently preventing the adsorption: the molecules of tetracycline cannot easily enter the small pores.

On the other hand, at high ionic strengths due to the "salting out" effect, hydrophobic interaction between the antibiotic molecules may overcome the repulsive electrostatic interaction, which favors the aggregation of the adsorbates. The formed aggregates may be large enough to block the pores, preventing other molecules from entering inside the silica gel. This would explain the decrease of the adsorption amount with the increase of the salt concentration.

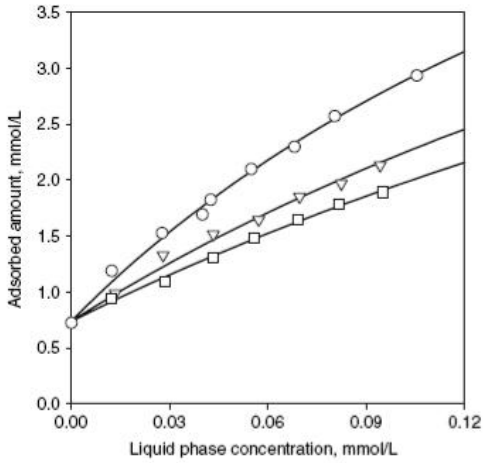

Figure 9. Effect of ionic strength on adsorption of tetracycline on silica (T = 296 K, pH = 6). Symbols: experimental data at 0.0001 M KCl (open circle), 0.01 M KCl (inverted triangle), and 0.1 M KCl (open square).

Cationic surfactants

The effect of the electrolyte on the adsorption of cationic surfactants on the nonionic XAD-16 polymer is shown in Fig. 10. In general, the electrolyte increases the adsorption of the surfactant due to the "salting out" effect. At the same time, the electrolyte influences the critical micelle concentration (CMC) of the surfactant. The driving force of

the micelle formation is hydrophobic interaction. The presence of electrolyte desolvates the surfactant molecules due to the "salting out" effect as a result of increased hydrophobic interaction. Also, the presence of electrolyte reduces the electrostatic repulsion between surfactant molecules due to the screening of the electric double layer charges. Thus, the presence of electrolyte substantially reduces the critical micelle concentration.

As one can see from the results (Fig. 10), the presence of electrolyte increases the adsorption of cationic surfactants, also shifting the plateau towards lower equilibrium concentrations. This can be explained by the decreased number of surfactant monomers in the bulk solution due to a decreased CMC. For the surfactant with a longer hydrocarbon chain, the salinity effect is more pronounced. Consequently, the adsorption amount even decreases at the highest ionic strengths [55].

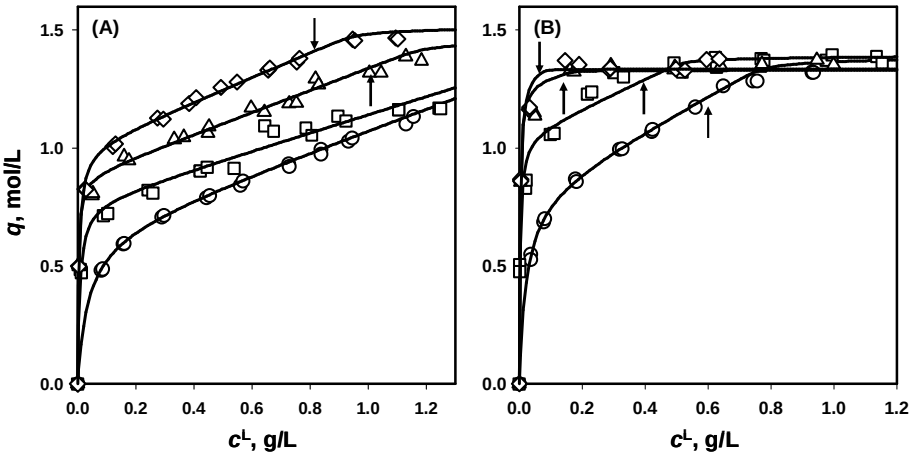

Figure 10. Adsorption isotherms of C_{12} (A) and C_{14} (B) on XAD-16 polymer at different electrolyte concentrations: 0.1 mmol/L (○); 5 mmol/L (□); 20 mmol/L (Δ); 40 mmol/L (◊). The vertical arrows show the measured CMC values. Solid lines: calculated with the Langmuir–linear model.

Adsorption of live bacteria

The influence of the ionic strength on the bacteria sorption onto a polymeric adsorbent was investigated using the bacteria *Bacillus cereus* and two anion-exchange polymeric adsorbents in Cl^- form. These data have not been published, although they are included in the thesis for the improved comprehension of adsorption phenomenon. The objective of this study was to investigate the removal of bacteria from aqueous solutions using polymeric adsorbents.

The bacterial cell surface charge originates from the dissociation or protonation of carboxyl, phosphate and amino groups, and consequently depends on the pH.

Table 4. Ionizable surface groups in various molecular species that are present on bacterial cell surfaces, and the $^{-}\log_{10}$ value of their dissociation constants (pKa) [59, 60, 61].

Group exists as	Located on	pKa
$-COOH \Leftrightarrow -COO^- + H^+$	Polysaccharide	2.8
	Protein, peptidoglucan	between 4.0 and 5.0
$-NH_3 \Leftrightarrow -NH_2^+ + H^+$	Protein, peptidoglucan	between 9.0 and 9.8
$-HPO_4 \Leftrightarrow -PO_4^- + H^+$	Teihoic acids	2.1
$-H_2PO_4 \Leftrightarrow -HPO_4^- + H^+$	Phospholipids	2.1
$-HPO_4^- \Leftrightarrow -PO_4^- + H^+$	Phospholipids	7.2

Table 4 presents possible chemical reactions charging the bacterial cell surface. A negative charge originates mainly from the dissociation or deprotonation of carboxyl, phosphate, and less commonly, sulfate groups in the cell wall. The positive charge is due

to amino groups of outer membrane layers. The net charge of the cell surface is determined by the negatively and positively charged groups on the bacterial cell surface, dependent on the surrounding conditions. At physiological pH values, i.e. between 5 and 7, most bacterial strains are negatively charged, as the number of carboxyl and phosphate groupes exceeds the number of amino groups.

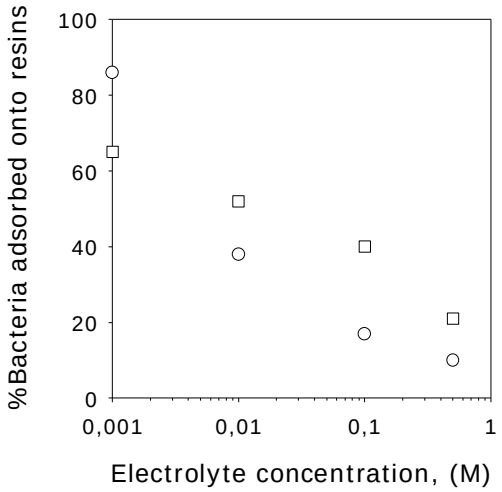

Figure 11. Effect of the ionic strength of the aqueous solution on the adsorption of bacteria onto anion exchange resins at room temperature: (□)=Dowex 66(Cl^-): *B. cereus*; (○)=Purolite A-835(Cl^-):*B. cereus.*

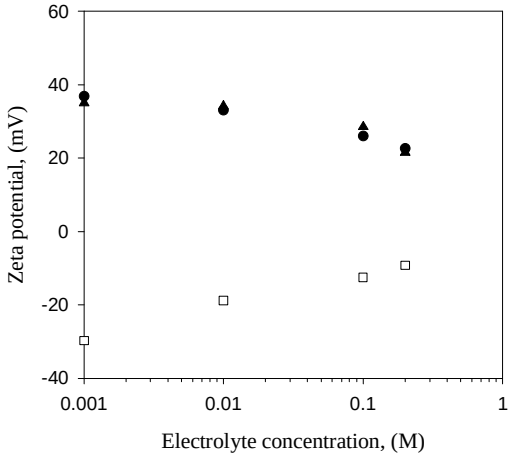

Figure 12. The zeta potential of the bacterial cells and the anion-exchange resins. (□) = *Bac. cereus*, (▲)= Dowex 66 (Cl^-), (●) = Purolite A–835 (Cl^-).

As seen in Fig. 11, the electrolyte plays a significant role in the bacteria adsorption. The fraction of the *B. cereus* bacteria adsorbed on the anion-exchange resins is relatively large at low electrolyte concentrations and monotonically decreases with an increase in the salt concentration. Based on the zeta potential measurements, the surfaces of the anion-exchange resins (Cl^- form) have a positive charge, while *B. cereus* cells have negatively charged cell surfaces (Fig. 12). As a result, the electrostatic interaction between the resins and the bacteria is strongly attractive.

It should be noted that electrostatic effects alone can explain neither the large difference in the adsorbed amounts, nor the fact that the adsorbed amounts decrease at different rates with an increasing ionic strength for both resins. One can see from Fig. 11 that, at a low ionic strength of the bulk liquid, more of *B. cereus* bacteria are adsorbed on the styrenic Dowex 66 resin than on the acrylic Purolite A835. Since the resins differ only slightly in their zeta potentials (Fig. 12), and therefore in their electrostatic interactions, the difference in the adsorption behavior must be attributed to the difference in the chemical

composition of the resins and, in particular, to their hydrophobicity or hydrophibicity. The matrix of the Dowex 66 resin contains aromatic rings, whereas the matrix of the Purolite A835 resin is acrylic. In absence of experimental hydrophobicity data for the resins, the inorganic/organic ratio of the matrix can give a rough idea of its hydrophobicity: the larger the value of this parameter, the more hydrophilic the surface of the resin. Matsuda et al. reported the inorganic/organic ratio for the matrices of styrenic and acrylic anion-exchangers, *i.e.* similar to those used in the present study, to be 0.14 and 1.69, respectively [62]. According to the contact angle measurements, the *B. cereus* bacteria cells are somewhat hydrophobic (29º contact angle for water). Therefore, we conclude that *B. cereus* exhibits more favorable hydrophobic interactions with the styrenic Dowex resin than with the acrylic Purolite resin. In other words, both electrostatic attraction and hydrophobic/hydrophilic interactions affect the bacterial adsorption on anion-exchange resins. The role of these factors depends on the electrolyte concentration of the medium.

Further inspection of the data in Fig. 11 shows that, at electrolyte concentrations of 0.01 and higher, the fraction of the *B. cereus* adsorbed on the hydrophobic resin (Dowex 66) is smaller than that adsorbed on the hydrophilic resin (Purolite A835). This apparent contradiction with the discussion above can be explained by considering the possibility of bacterial aggregation in the solution: aggregated bacteria have a more hydrophilic surface than that of the individual bacteria [62].

Table 5. Dependence of the bacterial co-aggregation on the electrolyte concentration.

c_{KCl}, mol/L	Absorbance, t=1 h	Absorbance, t=24 h
0.001	0.90785	0.29492
0.01	1.053	0.0594

The ability of bacteria to aggregate was investigated with the steady-state turbidity method. Obviously, the rate of the sedimentation of the aggregated bacteria is higher than that of non-aggregated ones. The results show that the absorbance in the measuring cell with bacteria resuspended in 0.001 M KCl after 24 hours was higher than in 0.01 M (Table 5). This means that the high electrolyte concentration promotes bacterial aggregation.

The aggregation possibility was also shown by the calculation of energy interaction between bacteria. In Appendix I the values of the energy of interaction between bacteria with the increasing ionic strength in liquid are presented. The calculation was based on the DLVO theory, according to which the repulsion between bacteria decreases with the increase of electrolyte concentration. The results show that at the highest salt concentrations (0.1 and 0.2 M KCl) adhesion between bacteria can be expected (see Appendix I).

3.1.3 **Effect of temperature on the adsorption**

In order to generate a better understanding of molecular interactions between the solutes and the adsorbent surface, the effect of the temperature on the adsorption was studied. In general, adsorption experiments with different temperatures are used for the evaluation of standard thermodynamic parameters associated with adsorption, such as Gibbs energy, $\Delta_{ads}G$, enthalpy, $\Delta_{ads}H$, and entropy, $\Delta_{ads}S$. The change in the standard free energy shows whether adsorption is spontaneous ($\Delta_{ads}G < 0$) or not ($\Delta_{ads}G > 0$). The magnitude of the standard enthalpy change indicates whenever the $\Delta_{ads}H$ of physical adsorption which is approximately 20 kJ/mol that of chemisorption is higher than 80 kJ/mol [1, 3, 4]. The standard entropy change ΔS indicates whether the system becomes more structured ($\Delta_{ads}S < 0$) or more random ($\Delta_{ads}S > 0$).

The theory for calculation of thermodynamic parameters is given in section 2. The results of the calculations are shown in Tables 6-8.

Table 6. Thermodynamic parameters of *β*-estradiol adsorption onto XAD-16, XAD-7, and GAC adsorbents.

Adsorbent	T (K)	$\Delta_{ads}G$ (kJ/mol)	$\Delta_{ads}H$ (kJ/mol)	$\Delta_{ads}S$ (J/mol K)
XAD-7	296	-9.2	-11	-0.3
	310	-9.8		
	323	-10.2		
XAD-16	296	-14.9	-26	-4.6
	310	-15.1		
	323	-14.4		
GAC	296	- 17.4	58	33
	310	- 18.9		
	323	- 21.5		

17 β-estradiol

The thermodynamic parameters of estradiol adsorption on the polymeric adsorbents and activated carbon are shown in Table 6. The negative values of Gibbs energy indicate spontaneous adsorption for all adsorbents. Negative enthalpy values for the polymeric adsorbents indicate that the adsorption is exothermic. The positive value of enthalpy changes in the activated carbon adsorption process indicates that the adsorption process is endothermic, unfavorable, and therefore, entropy driving. Generally, physical sorption involves an enthalpy change is approximately 20 kJ/mol, while the enthalpy change value of chemisorption remains between 80–200 kJ/mol [4]. The results obtained for XAD-7 and XAD-16 are –11 kJ/mol and –26 kJ/mol, respectively, indicating that the adsorption is physical and involves weak forces of attraction. The enthalpy value for activated carbon sorption is 58 kJ/mol, which indicates that the adsorption is rather chemical or transitional, i.e. between physical and chemical sorption. The results also show that the entropy change during adsorption onto activated carbon was positive. It should be noted that Gibbs energy is derived from the balance between $\Delta_{ads}H$ and $T\Delta_{ads}S$ values

($\Delta G = \Delta H - T\Delta S$). The negative values of Gibbs energy at all three temperatures mean that the entropic driving force not only contributes to the adsorption, but is also sufficiently large to overcome the unfavorable endothermic nature of the adsorption process resulting in a significantly negative Gibbs free energy (Table 6). The entropic driving forces are associated with the displacement of the water molecules surrounding the solute molecules. The total entropy of the system is the sum of the entropy of the solutes and that of the solvent molecules. The change of the solute entropy due to adsorption is always negative. However, the solvent molecules, which surround the solute molecules in the liquid phase, are restructured during adsorption. The positive $\Delta_{ads}S$, observed for activated carbon, actually originates from the increasing entropy of the solvent. The cause of the negative $\Delta_{ads}S$ for adsorption on the XAD polymers is that the entropy of the solutes decreases more than the entropy of the solvent increases.

Table 7. Thermodynamic parameters of tetracycline adsorption on silica at pH 6 and an ionic strength of 0.1 mM KCl.

T (K)	$b \cdot Q_{rev,-}$	$\Delta_{ads}G$ (kJ/mol)	$\Delta_{ads}H$ (kJ/mol)	$\Delta_{ads}S$ (J/molK)
296	29.75	–8.354	–15.80	–25.10
303	26.03	–8.214		
310	22.27	–8.002		

Tetracycline

The thermodynamic parameters of antibiotic tetracycline adsorption on silica are shown in Table 7. The negative Gibbs energy value indicates that the adsorption is spontaneous, and from the negative and small (< –20 kJ/mol) value of the enthalpy it can be concluded that the adsorption was exothermic and physical. The negative adsorption entropy indicates a decreased randomness at the solid/solution interface during adsorption. It should be noted that the thermodynamic parameters were calculated only for reversible adsorption sites.

Cationic surfactants

Since the adsorption of surfactants is a two-step process involving a) monolayer forming and b) aggregation on the surface, thermodynamic parameters were evaluated for each step. The thermodynamic parameters of the surfactants adsorption are summarized in Table 8.

The estimated negative Gibbs energies indicate spontaneous adsorption for both the first layer and the surface aggregates. For the surfactant having a longer hydrocarbon chain, the adsorption is stronger that is in agreement with other studies [63]. Table 8 also demonstrates that the adsorption of monomers on the surfaces is more favorable than the formation of hemimicelles ($\Delta_{ads}G_1$ is more negative than $\Delta_{ads}G_2$). The enthalpy of the adsorption is exothermic for both stages of adsorption. The calculated magnitudes of the enthalpy values indicate the physical sorption of the surfactants. The entropy change values show that hemimicelles are more structured than the first layer ($\Delta_{ads}S_2$ is more negative than $\Delta_{ads}S_1$).

Table 8. Thermodynamic parameters for adsorption of C_{12} and C_{14} homologues of benzalkonium chloride on XAD-16. Background electrolyte: 0.1 mM NaCl. The subscript 1 refers to adsorption on the surface and subscript 2 to the formation of aggregates.

BKC homologue	T	$\Delta_{ads}H_1$ kJ mol^{-1}	$\Delta_{ads}S_1$ J mol^{-1}K^{-1}	$\Delta_{ads}G_1$ kJ mol^{-1}	$\Delta_{ads}H_2$ kJ mol^{-1}	$\Delta_{ads}S_2$ J mol^{-1}K^{-1}	$\Delta_{ads}G_2$ kJ mol^{-1}
C_{12}	296			-21.55			-13.38
	310	–19.92	+5.5	-21.62	–17.33	–13.33	-13.19
	323			-21.69			-13.02
C_{14}	296			-23.51			-14.13
	310	–25.64	–7.2	-23.41	–22.88	–29.56	-13.72
	323			-23.31			-13.34

The cost of the regeneration of the spent adsorbent plays an important role in choosing the adsorbent. The calculation of thermodynamic parameters may give important information about the type of adsorption (physical sorption or chemisorption), which determines the method of regeneration of the adsorbent.

For the studied systems, it was found that the adsorption of estradiol and surfactants onto polymeric adsorbents was due to physical sorption ($\Delta_{ads}H$ were smaller than 26 kJ/mol by its absolute value). The adsorption enthalpy changes of estradiol on activated carbon had positive sign. The adsorption enthalpy magnitude 58 kJ/mol corresponds rather to chemisorption than to physical sorption. The chemical sorption can be attributed to the possible alteration of the chemical nature of the adsorbate due to chemical reaction with the adsorbent surface. Thus, after the chemisorption, the original adsorbate species cannot be recovered. The regeneration of the loaded adsorbent in this case may be possible only under in extreme temperature or with suitable chemical treatment of the surface. On the other hand, the regeneration of polymeric adsorbents with physically loaded solutes can be achieved under milder condition.

3.1.4 **Influence of organic solvent on the adsorption**

This part of the study was performed to acquire additional information on the regeneration of the adsorbents. It was expected that ethanol is able to reduce the dielectric constant of the solvent and, thereby, reduce the adsorbed amount, or at sufficiently high concentration to complete prevent the adsorption process [64].

The results of the study were described in the attached Papers II and V. The results showed that the presence of ethanol remarkably reduces the adsorbed amounts of all solutes onto all types of adsorbents (Figs. 1 and 2 in Paper II and Figs. 1-3 in Paper V). It was also observed that ethanol itself adsorbs onto polymer, and can thereby displace surfactants from the adsorbent surface. However, the amount of adsorbed ethanol was negligible in the comparison of adsorbed amounts of surfactants (Fig. 3 in Paper II).
The importance of this study was in the evaluation of equilibrium parameters, which were used for the elution curves design in the Section 3.3.

3.2 ADSORPTION OF AGGREGATING MOLECULES

As it was shown in the experiments, the aggregation phenomena of adsorbed compounds play significant role on the adsorption extent. For an adsorbent with small pores, such as silica gel, the aggregation of the molecules in the bulk and on the surface may reduce adsorption due to the blocking of the pores (see Section 3.1.2 and Paper I).

As it was shown in Section 3.1.2, the aggregation of bacteria during adsorption has an influence to the adsorption extent. Because of the decrease of hydrophobicity in the bacteria in the aggregated state, the amount of the adsorbed bacteria is larger for the more hydrophilic adsorbent at a higher degree of aggregation (at a higher ionic strength), than for the hydrophobic one (Fig. 11).

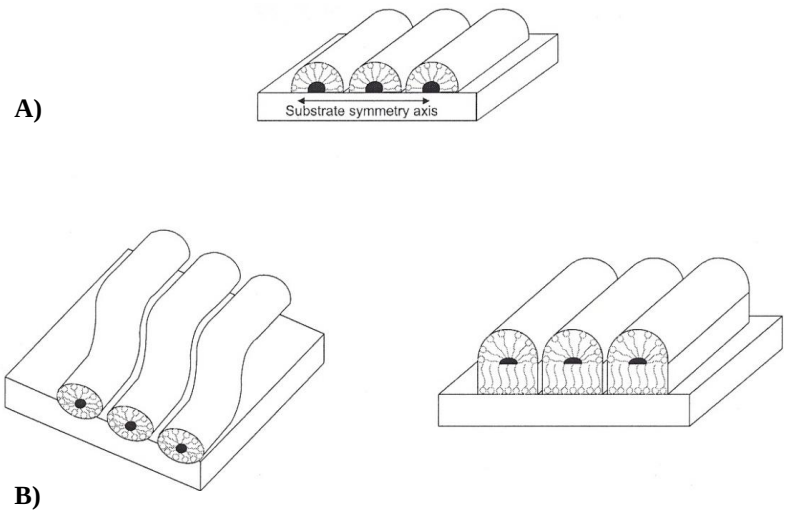

Figure 13. Models of layers of a cationic surfactant at solid/liquid interfaces: A) hydrophobic surface: hemicylindrical aggregates; B) hydrophilic surfaces: (*left*) flexible cylindrical aggregates, (*right*) monolayer topped with hemicylinders [1].

In this study, the influence of the aggregation (micellization) phenomenon of surfactants on adsorption is described in the example of the cationic surfactant BKC. Surfactants are the surface-active molecules with hydrophobic and hydrophilic parts. In aqueous solutions, they exist as free monomers below the CMC, and due to their amphipathic molecular structure, they form aggregates in the solution and on interfaces at concentrations equal to the CMC and higher. The driving force of this aggregation or micelle formation is hydrophobic interactions between hydrocarbon chains of surfactant molecules [65]. Micelle formation poses additional difficulties for describing the surfactant adsorption equilibrium at concentration values below and above the CMC.

The adsorption behavior of ionic surfactants on a solid surface has been investigated extensively. Adsorption of cationic surfactants onto solid surfaces typically displays two-step adsorption mechanism as a function of surfactant concentration. At low concentrations the adsorption driven forces depend on the nature of the natures of adsorbent and adsorbate. With the increasing of the liquid phase concentration, adsorbate density on the adsorbent surface also increases until the surfactant achieves its critical micelle concentration, after that lateral hydrophobic interaction between adsorbed molecules becomes predominant. At low equilibrium concentrations, individual molecules adsorb onto silica surface [51, 66] and metal oxides, such as alumina oxide and titanium oxide [67, 68] due to electrostatic interaction. The dsorption of cationic surfactant onto nonionic graphite surface was due to hydrophobic interaction [69]. The adsorption onto ion-exchange materials such as zeolite clinoptilolite [63] and clay [70] was due to ion-exchange mechanism. In the adsorption onto activated carbon an ion-exchange mechanism and an ion pairing were predominant [71]. At a sufficiently high liquid phase concentration - the CMC and higher - surfactants form aggregates on solid surfaces [55, 63, 66-71].

A step forward in understanding the surfactant adsorption was made by Manne et al. [69], when they first showed the direct imaging of saturated surfactant layers adsorbed onto hydrophobic surface. They found that at low concentrations the surfactant molecules

form monolayer periodic structures, which are twice the molecular length and placed a head-to-head and tail-to-tail. They also postulated that this monolayer structure serves as a template for hemimicelle formation as the concentration is increased. Before that, the surface aggregation was only proposed in order to explain the specific shape of the surfactant adsorption isotherms.

The various micelle structures, including bi-layers, hemicylinders and spheres, have been observed to be dependent on the nature of the surfactant and surfaces (Fig. 13) [1, 62, 69, 72-78].

Several models were used for the describing the two-step adsorption of surfactants onto a solid surface. Zhu and Gu [79] used their model for fitting the adsorption isotherms where two-step adsorption was modeled with two binding constants (Eq. 14). The first step is described with the Langmuir isotherm. The second takes into account the surface aggregation, where each molecule of the monolayer acts as an "active center" for aggregation with the increasing surface density of surfactant. This model reproduces both Langmuir and S-shaped adsorption isotherms common in the adsorption of surfactants. The limitation of this model is in the difficulty the parameters correlate at low values of aggregates number (n):

$$q = \frac{q_s b_1 c \left(n^{-1} + b_2 c^{n-1} \right)}{1 + b_1 c + b_1 b_2 c^n} \qquad (14)$$

Another model, the self-consistent field (SCF) lattice theory, is has been successfully used for the surfactants adsorption on a charged surface. Also, it interprets quite well the adsorption with variable ionic strengths and pH values [68, 80].

This thesis presents a simplified adsorption model, describing the formation of surface aggregates. Again, this model describes two-step surfactant adsorption, where single molecules adsorb directly on the adsorbent surface, forming the first monolayer. This step

is described with the Langmuir isotherm model. The model assumes the monolayer adsorption (each site can accommodate only one molecule), the adsorption energy is the same at all sites, the adsorbent has finite adsorption capacity, and there is no interaction between adsorbed molecules [2]. Each molecule in the first layer can act as an active centre (or site), onto which a surface aggregate can grow (Fig. 13 (A)). Assuming that the interaction energy between the molecules in the liquid phase and the surface aggregate is constant, and that the number of molecules in the surface aggregate is unlimited, this distribution can be described with a linear isotherm. The total amount of surfactant adsorbed, q, is the sum of the molecules in the first layer and in the aggregates, and can thus be written as

$$q = \frac{q_s b_1 c}{1 + b_1 c} + \frac{q_s b_1 b_2 c^2}{1 + b_1 c} = \frac{q_s b_1 c}{1 + b_1 c}\left(1 + b_2 c\right) \tag{15}$$

For the details, see Paper III.

Simultaneous micellization and adsorption equilibria

In this example, the evaluation steps for an apparent adsorption equilibrium with simultaneous micellization are discussed.

Surfactants form micelles at their CMC and higher concentrations. Micelle formation creates additional complication in the simulation of the surfactant adsorption equilibrium. The calculation example given can be used in the description of surfactant adsorption at concentrations exceeding the CMC. Firstly, the mass fraction of micelles (x) and the total mass of the surfactant (w) in the liquid phase were calculated from the mass balance and presented in Fig. 14(A). This enables the calculation of the concentration of the surfactant free monomers (c_A^L) at any surfactant concentration in the liquid phase (w_0) (Fig. 14(B)). As can be seen from the figure, at the w_0 concentration the plot shows a plateau due to micellization when the monomer concentration does not change. It means that the adsorption isotherm in Fig. 14(C) does not rise after the monomers concentration reaches approximately 0.8 mmol/L. The last picture shows the apparent adsorption isotherm,

where both surfactant micellization and adsorption were taken into account. This isotherm shows that the plateau after the liquid phase surfactant concentration is equal or close to the CMC. This is because only monomers adsorb onto the solid phase, whereas micelles stay in the bulk solution.

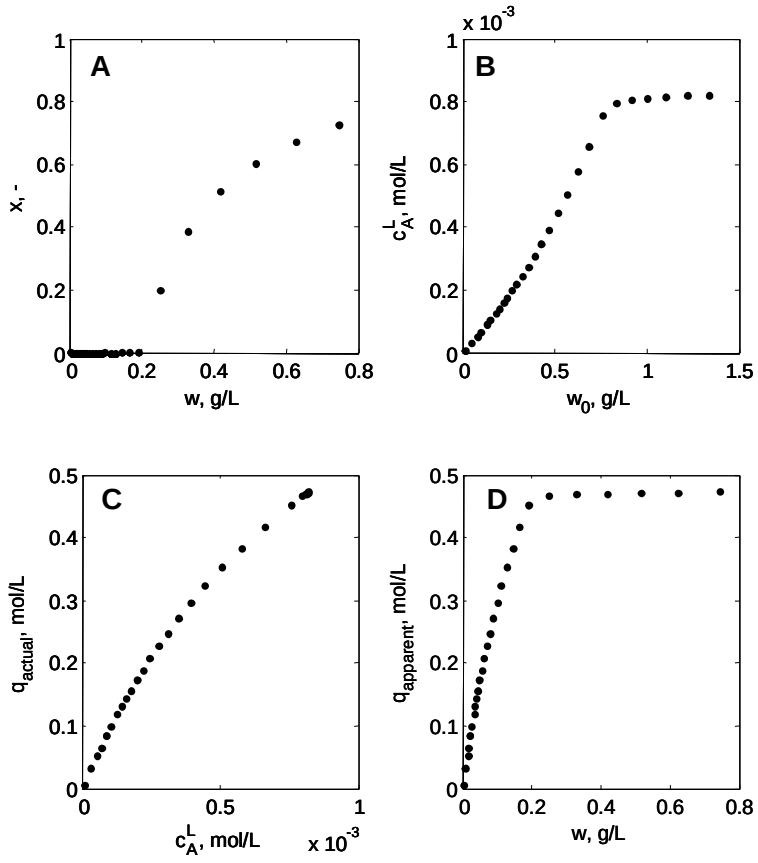

Figure 14. (A) The mass fraction of surfactants in the micelles (x) *vs*. the total mass of surfactants in the liquid phase; (B) the molar concentration of free monomers in the liquid phase *vs*. the initial mass of the surfactant; (C) the adsorption isotherm of the surfactant without micellization taken into account; (D) the adsorption isotherm where the micellization of the surfactant is taken into account.

3.3 PROCESS PERFORMANCE

This section illustrates how the performance of adsorptive separation processes can be analyzed and quantified. As the first example, the adsorptive removal of the commercial surfactant BKC using a polymeric adsorbent is discussed (Paper II). As the second example, the recovery of glucose from a hydrolyzate containing fermentation inhibitors, such as furfural, hydroxymethylfurfural, and acetic acid, is discussed (Paper V).

The adsorptive removal (separation) of solutes from aqueous solutions is usually operated as a periodic system where the loading step is followed by the regeneration step. The regeneration may be intensified by the implying suitable organic solvent as a desorbate.

The adsorption removal of the commercial cationic surfactant BKC from an aqueous solution was studied by using the non-ionic polymeric adsorbent XAD-16. Firstly, the polymeric adsorbent was loaded with the surfactant so that the breakthrough curve was obtained (Fig. 15). As one can see from the figure, the adsorption capacity was large: the saturation was reached after 200 BV. However, the effective removal capacity is considerably lower than the saturation capacity: approximately 80 BV could be processed for the outlet concentration $c/c^{feed} \leq 0.10$. For the regeneration of the adsorbent loaded with the surfactant, pure water and water-organic solvent mixture were applied. As it was expected, the regeneration with water took rather a long time: the outlet profile decreased monotonically and extended over thousands of BV (Fig 16). The regeneration step was intensified by using an ethanol-water mixture as a desorbate. As can be seen in Fig. 16, a 50-wt % ethanol-water solution was the most effective: a steep concentration profile of the surfactant with a short tail was observed. Approximately 20 BV were needed for the total removal of the surfactant form the adsorbent bed. After the regeneration, the polymer was washed with pure water for the removal of ethanol. The duration of this step was roughly 2 BV (Fig. 10 in Paper II).

The relative duration of each step within one process cycle – loading, regeneration, and washing – is shown in Fig. 11 in Paper II. The duration criterion of the loading step was $c/c^{feed} \leq 0.10$; the regeneration was carried out with a 50 wt-% ethanol-water solution. According to this figure, the loading step comprised close to 82% of the complete cycle, 16% regeneration, and 2% washing.

The relationship between the removal percentage and the productivity of the process is illustrated in Fig. 17. The productivity was defined as the duration of the loading step relative to the complete process cycle. As can be seen, the productivity decreases gradually with the increasing removal percentage until approximately 95%. After that, the productivity falls rapidly. Lowering the surfactant removal percentage had a positive effect on productivity (Fig. 17A) since the duration of the regeneration and washing steps were not affected by the level of loading of the adsorbent. The rapid decrease in the PR% at a high *R*% range can be observed in Fig. 17B. Thus, the cost of the adsorption process is proportional to the purity of the final product (Fig. 17A).

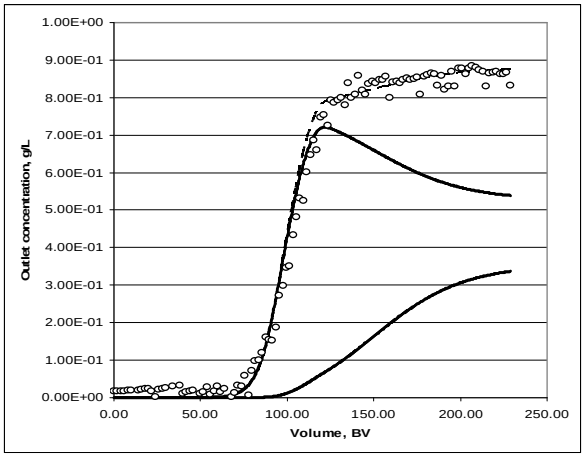

Figure 15. Adsorption of C_{12} and C_{14} on XAD–16 in a column. Flow rate 2 BV/h. Symbols: experimental data; solid lines: predicted C_{12} and C_{14} (higher is C_{12}), dashed line: C_{12} and C_{14} mixture.

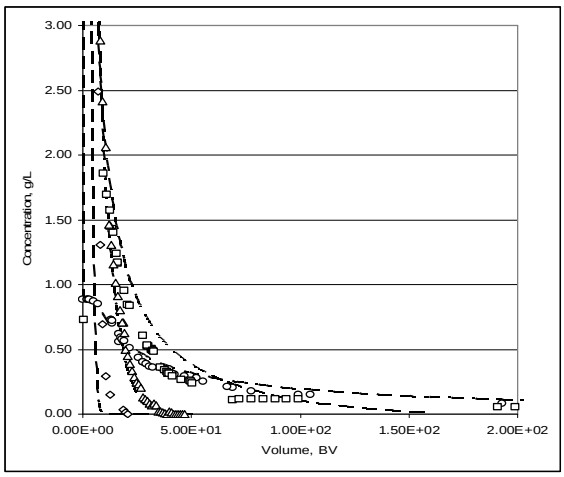

Figure 16. Regeneration of the column with aqueous ethanol. Circles: water, squares: 20 wt-% EtOH, triangles: 35 wt-% EtOH, diamonds: 50 wt-% EtOH. Dashed lines: total concentration of surfactants (C_{12}+C_{14}=BKC) predicted by using the column model.

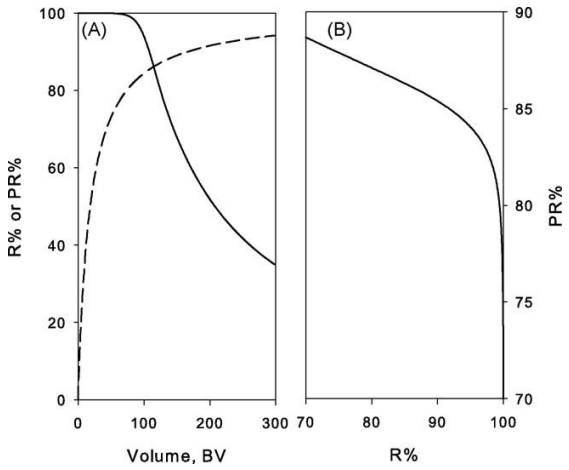

Figure 17. Performance of an adsorptive removal of the surfactant. (A) Influence of the duration of the loading step (BV) on surfactant removal percentage (R%, solid line) and productivity (PR%, dashed line). (B) The influence of the removal percentage on productivity. Flow rate 2 BV/h, regeneration with a 50 wt% ethanol solution.

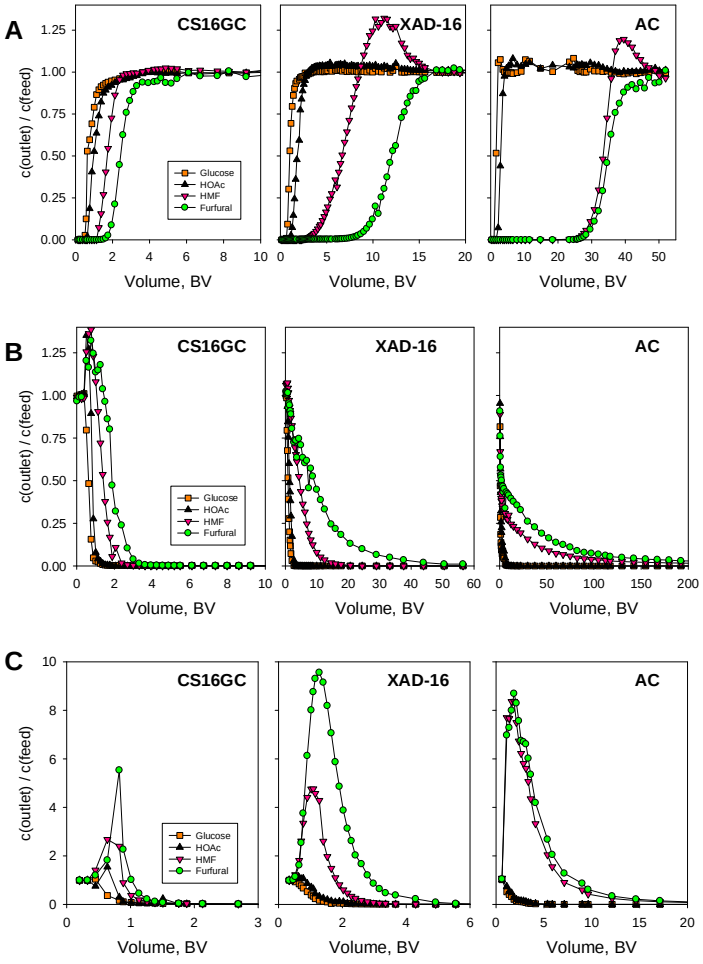

Figure 18. Column dynamics experiments. (A) Loading of an empty bed from a 20 wt-% sulfuric acid solution, (B) regeneration with water after loading step, (C) regeneration with a 50 wt-% ethanol-water solution after the loading step. Symbols: (□) glucose, (Δ) acetic acid, (Δ) HMF, (○) furfural.

Fig. 18 shows the column loading – the elution experimental data of glucose, furfural, hydroxymethylfurfural, and acetic acid for polymeric adsorbents, CS16GS and XAD-16, and activated carbon [Paper V]. Using the experimental data, in order to estimate the most effective adsorbent for the separation of glucose from the inhibitors, the process performance was calculated and presented in Figs. 19 and 20. Fig. 19A shows the influence of the loading step duration on the amount of inhibitors removed. As can be seen, the activated carbon has the highest adsorption capacity (Fig. 19A) and, consequently, the longer loading step duration. In Fig. 19B presents the productivities of adsorbents with the regeneration step taken into account. The productivity of the CS16GS polymer was the highest for both methods of regeneration, the water and ethanol-water solutions. As can be seen in Fig. 18, the regeneration of CS16GS was fast: approximately 4 BV of water and 2 BV of ethanol-water adsorbate were needed for the desorption of the most adsorbed solute furfural. The activated carbon productivity was worse because of strongly adsorbed solutes: hundreds of BV of water or 20 BV of ethanol-water mixture were needed for activated carbon regeneration. The XAD-16 polymer was highly productive with organic solvent regeneration.

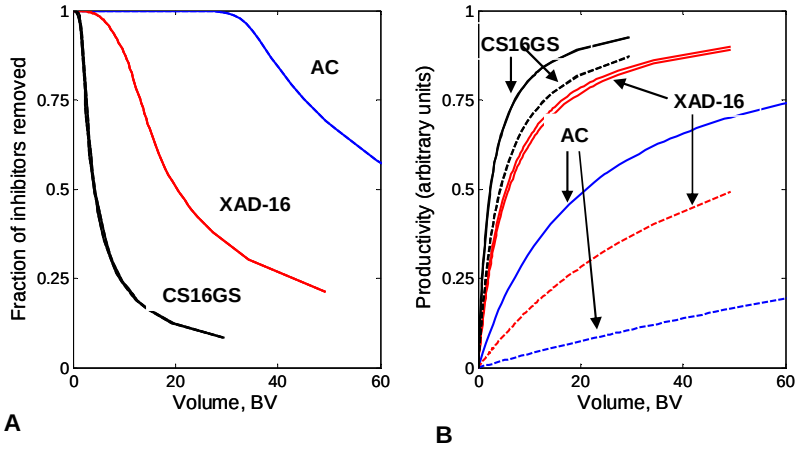

Figure 19. Performance of the cyclic separation of fermentation inhibitors processes. (A) calculated based on loading step data, (B) calculated based on loading-elution data.

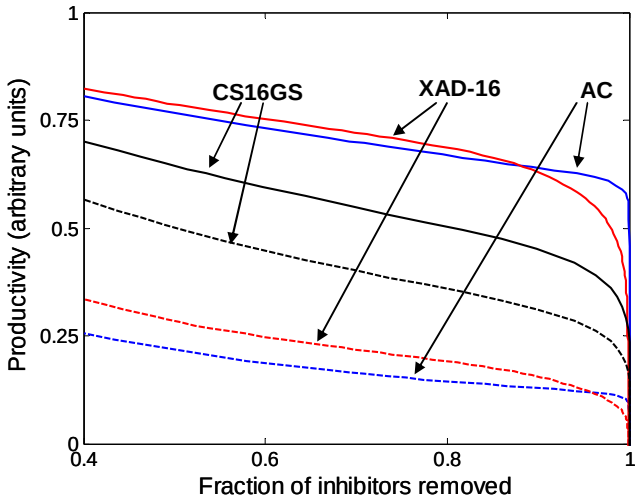

Figure 20. Influence of inhibitors removal percentage on productivity. Lines: regeneration with ethanol-water solution (solid), regeneration with pure water (dashed).

All process performance parameters need to be considered when evaluating the applicability of the adsorbent to the separation/adsorption process. For the adsorbent, having a high capacity does not always show the best productivity and vice versa. Fig. 20 represents the inhibitors separation performance when the productivity of the adsorbents depends on the fraction of inhibitors removed. In this example, it can be detected that adsorbents with the smallest adsorption affinity towards inhibitors (CS16GS) had the highest productivity in the case of regeneration with water, which is the least costly regeneration method. Activated carbon and XAD-16 adsorbents had a much higher capacity than CS16GS and showed higher productivity, but they were regenerated by a more expensive desorbate, a 50 wt% ethanol-water solution. Also, Fig. 18 shows that the productivity of activated carbon was the highest for the higher degree of inhibitors removal.

4 CONCLUSIONS

The applicability of different types of adsorbents for the adsorptive removal of organic solutes from aqueous solutions was studied. It was shown that cationic surfactants had a high affinity towards the nonionic polymeric adsorbent Amberlite XAD-16. Their adsorptive capacity was high. However, large intraparticle mass transfer resistance decreases the dynamic adsorption capacity. According to the calculated thermodynamic parameters, it was shown that the adsorption of the surfactants had physical nature. It was demonstrated that a loaded adsorbent could be more easily regenerated by using an organic solvent.

Three adsorbents were studied for the removal of inhibitors from the reconstituted acid hydrolyzate of lignocelluloses. The results show that activated carbon and a neutral polymer adsorbent had higher productivity than an ion-exchange resin when an ethanol-water mixture was used as the regeneration agent. However, the productivity of the process was higher with the ion-exchange resin when pure water was used as the desorbate. It was also found that none of the adsorbents could separate sucrose and acetic acid.

In this thesis, the fundamental phenomena such as the influence of acidity, ionic strength, and temperature on adsorption were also studied. Ionic strength was found to be an important parameter for surfactants. Hydrophobic interactions were the main driving forces for the adsorption of the surfactant on XAD-16. Hydrophobic interactions were the main driving forces for micellization. Increasing the salt concentration in the liquid phase was found to promote surfactant adsorption. Also, the presence of salt decreased the CMC that, in turn, decreased the adsorbed amount of surfactant.

In the example of a gel-type adsorbent, silica, it was shown that the aggregation of a solute, antibiotic tetracycline, decreased the adsorption affinity because aggregates could

not penetrate the pores of the silica. No such changes were observed for the macroporous non-ionic adsorbent and neutral molecule estradiol with an increasing salt concentration. The results of ionic strength dependence change the binding affinity of living bacteria on hydrophilic and hydrophobic adsorbents. The aggregation of bacteria decreases the hydrophobicity and thereby increases the adsorption affinity to the hydrophilic adsorbent.

A pH dependence was observed for solutes with acid-base properties. The adsorption of tetracycline onto silica particles was strongly pH dependence. It was shown that the predominant mechanism of adsorption was hydrogen binding and an increasing pH also increased the negative charges of both the adsorbate and the adsorbent. Also, an increase in pH changed the attractive adsorption forces between activated carbon and estradiol into repulsive ones. As a result, adsorption decreased dramatically. On the other hand, the adsorption affinity did not change between non-ionic polymeric adsorbents and estradiol molecules.

The dependence of adsorption on temperature studied in this work provided the data for calculation of thermodynamic parameters of the adsorption, which makes available the approaching to the interactions character involved in the adsorption. It was shown that a decreasing in temperature favored the adsorption of surfactant onto polymeric adsorbents. The nature of the Gibbs energy changes and enthalpy were associated with favorable physical sorption. Also, the adsorption of estradiol onto a polymeric adsorbent was favorable and physical. However, the adsorption of estradiol onto activated carbon was chemical nature due to the high enthalpy value. The adsorption of tetracycline onto silica particles was also physical and favorable. However, on the basis of the isotherms shape it was observed that the adsorption was irreversible.

REFERENCES

1. Bellmann C., Chapter 12 Surface Modification by Adsorption of Polymers and Surfactants, In: Polymer surfaces and Interfaces, Springer-Verlag, Berlin, 2008, p. 235–259.
2. Ruthven D.M., Principles of Adsorption and Adsorption Processes, John Wiley & Sons, New York, 1984.
3. Atkins P.W., Physical sorption, 2 d Edition, Oxford University Press, 1982.
4. Liu Y., Liu Y.-J., Biosorption isotherms, kinetics and thermodynamics, *Separation and Purification Technology*, 61 (2008) 229–242.
5. Bandosz T.J., Activated Carbon Surface in Environmental Remediation, 1 st Edition Elsevier LTD, Netherlands, 2006.
6. Yang R.T., Adsorbents: Fundamentals and application, John Wiley & Sons, Inc, Hoboken, New Jersey, 2003.
7. Gupta V.K., Carrott P.J.M., Ribeiro Carrott M.M.L., Suhas, Low-Cost Adsorbents: Growing Approach to Wastewater Treatment–a Review, *Environment Science and Technology*, 39 (2009) 783–842.
8. Nemerow N.L., Dasqupta A., Industrial and hazardous waste treatment, Van Nostrand Reinhold, New York, 1991.
9. Steart M., Sweetland L.A., Horner D.J., Removal of pesticides from water using hypercrosslinked polymer phases: Part 4–Regeneration of Spent Adsorbents, *Trans IChemE*, 76 (1998) 142–150.
10. Mollah A.H., Robinson C.W., Pentachlorophenol adsorption and desorption characteristics of granular activated carbon – I. isotherms, *Water Research*, 30 (1996) 2901–2906.
11. Kilduff E.J., King C.J., Effect of carbon adsorbent surface properties on the uptake and solvent regeneration of phenol, *Industrial Engineering Chemistry*, 36 (1997) 1603–1611.

12. Chern J.-M., Chien Y.W., Competitive adsorption of benzoic acid and *p*-nitrophenol onto activated carbon: isotherm and breakthrough curves, *Water Research*, 37 (2003) 2347-2356.
13. Okawa K., Suzuki K., Takeshita T., Nakano K., Regeneration of granular activated carbon with adsorbed trichloroethylene using wet peroxide oxidation, *Water Research*, 41 (2007) 1045-1051.
14. Backhaus W. K., Klumpp E., Narres H.-D., Schwuger M. J., Adsorption of 2,4-dichlorophenol on montmorillonite and silica: Influence of nonionic surfactants, *Journal Colloid and Interface Science*, 242 (2001) 6–13.
15. Curkovic L., Cerjan-Stefanivic S., Filipan T., Metal ion exchange by natural and modified zeolites, *Water Research*, 31 (1997) 1379–1382.
16. Guo Z., Zheng S., Zheng Z., Separation of *p*-chloronitrobenzene and *o*-chloronitrobenzene by selective adsorption using Silicalite-1 zeolite, *Chemical Engineering Journal*, 155 (2009) 654–659.
17. Zeng Y.P., Ju S.G., Adsorption of thiophene and benzene in sodium-exchange MFI- and MOR-type zeolites: a molecular simulation study, *Separation and Purification Technology*, 67 (2009) 71–78.
18. Guo Z. B., Zheng S. R., Zheng Z., Jiang F., Hu W. Y., Ni L. N., Selective adsorption of *p*-chloronitrobenzene and *o*-chloronitrobenzene using HZSM-5 zeolite, *Water Research*, 39 (2005) 1174–1182.
19. Wang S., Huiting L., Xie S., Shenglin L., Longya X., Physical and chemical regeneration of zeolitic adsorbents for dye removal in wastewater treatment, *Chemosphere*, 65 (2006) 82–87.
20. Yu Y., Zhuang Y.-Y., Wang Z.-H., Adsorption of water-soluble dye onto functionalized resin, *Journal in Colloid and Interface Science*, 242 (2001) 288–293.
21. Pan B., Pan B., Zhang W., Zhang Q., Zhang Q., Zheng S., Adsorptive removal of phenols from aqueous phase by using a porous acrylic ester polymer, *Journal of Hazardous Materials*, 157 (2008) 293–299.

22. Juang J.Y., Shiau J.Y., Adsorption isotherms of phenols from water anto macroreticular resins, *Journal Hazardous Materials B*, 70 (2001) 171-183.
23. Yang W.B., Li A., Fan J., Yang L., Zhang Q., Adsorption of branched alkylbenzene sulfonate onto styrene and acrylic ester resins, *Chemosphere*, 64 (2006) 984–990.
24. Abburi K., Adsorption of phenol and *p*-chlorophenol from their single and bisolute aqueous solutions on Amberlite XAD–16 resin, *Journal of Hazardous Materials*, 105 (2003) 143–156.
25. Kujawski W., Warszawski A., Ratajczak W., Porębski T., Capała W., Ostrowskab I., Application of pervaporation and adsorption to the phenol removal form wastewater, *Separation and Purification Technology*, 40 (2004) 123–132.
26. Clara M., Scharf S., Scheffknecht C., Gans O., Occurrence of selected surfactants in untreated and treated sewage, *Water Research*, 41 (2007) 4339–4348.
27. Helfferich F., Ion Exchange, Dover Publications, Inc., New York, 1995.
28. http://www.tradett.com/selloffer_dir/482/Adsorbents.html
29. Faust S.D., Osman M.A., Adsorption Processes for Water Treatment, Butterworth Publisher, 1987.
30. Mes T., Zeeman G., Lettinga G., Occurrence and fate of estrone, 17 β-estrediol and 17 α-ethynylestradiol in STPs for domestic wastewater, *Reviews in Environmental Science and Bio/Technology*, 4 (2005) 275-311.
31. Rabølle M., Spliid N.H., Sorption and mobility of metronidazole, olaquinodox, oxytetracycline and tylosin in soil, *Chemosphere*, 40 (2000) 715–722.
32. Kümmer K., Pharmaceuticals in the Environment, Second Edition, Springer-Verlag Berlin Heidelberg, 2004.
33. Scott M.J., Jones M.N., The biodegradation of surfactants in the environment, *Biochim. Biophys. Act*, 1508 (2002) 235–251.

34. Halling-Søresen B., Nors Nielsen S., Lanzky P.F., Ingerslev F., Holten Lützhøft H.C., Jørgensen S.E., Occurrence, Fate and Effects of Pharmaceutical Substances in the Environment – A Review, *Chemosphere*, 36 (1998) 357–393.
35. Sören T.-B., Pharmaceutical antibiotic compounds in soils – a review, *J. Plant Nutr. Soil Sci*., 166 (2003) 145–167.
36. Kim S.D., Jaeweon C., Kim I.S., Vanderford B.J., Snyder S.A., Occurrence and removal of pharmaceuticals and endocrine disruptors in South Korean surface, drinking, and waste waters, *Water research*, 41 (2007) 1013–1021.
37. Khanal S.K., Xie B., Thompson M.L., Sung S., Ong S–K., Van Leeuwen J., Fate, Transport, and Biodegradation of Natural Estrogens in the Environment and Engineered Systems, *Environmental Science & Technology*, 40 (21) (2006) 6537–6546.
38. Rodgers-Gray T.P., Kelly C., Morris S., Brighty G., Waldock M.J., Sumpter J.P., Tyler C.R., Exposure of Juvenile Roach (*Rutilus rutilus*) to Treated Sewage Effluent Induces Dose-Dependent and Persistent Disruption in Gonadal Duct Development, *Environmental Science & Technology*, 35 (2001) 462–470.
39. Jenkins R.L., Wilson E.M., Angus R.A., Howell W.M., Kirk M., Moore R., Nance M., Brown A., Production of Androgens by Microbial Transformation of Progesterone *in Vitro*: A Model for Androgen Production in Rivers Receiving Paper Mill Effluent, *Environmental Health Perspectives*, 112 (15) (2004) 1508–1511.
40. Ahmed S.A., The immune system as a potential target for environmental estrogens (endocrine disrupter): a new emerging field, Toxicology, 150 (2000) 191–206.
41. Mendes J.J.A., The endocrine disrupters: a major medical challenge, *Food and Chemical Toxicology*, 40 (2002) 781–788.

42. Berg C., Halldin K., Brunström B., Brandt I., Methods for studying xenoestrogenic effects in birds, *Toxicology Letters*, 102–103 (1998) 671–676.
43. Taherzadeh M.J., Karimi K., Acid-based hydrolysis processes for ethanol from lignocellulosic materials, *BioResources*, 2 (3) (2007) 472- 499.
44. Larsson S., Palmqvist E., Hahn-Hägerdal B., Tengborg C., Stenberg K., Zacchi G., Nilvebrant N.-O., The generation of fermentation inhibitors during dilute acid hydrolysis of soft wood – Anion accumulation versus uncoupling, *Enzyme and Microbial Technology*, 24 (1999) 151-159.
45. Mussato S.I., Roberto I.C., Alternatives for detoxification of diluted-acid lignocellulosic hydrolyzates for use in fermentative processes: a review, *Bioresource Technology*, 93 (2004) 1–10.
46. Delgenes J., Moletta R., Navarro J.M., Effects of lignocellulose degradation products on ethanol fermentations of glucose and xylose by Saccharomyces cerevisiae, Zymomonas mobilis, Pichia stipitis, and Candida shehatae, *Enzyme and Microbial Technology*, 19 (1996) 220-225.
47. Nigam J.N., Ethanol production from wheat straw hemicellulose hydrolysate by Pichia stipitis, *Journal of Biotechnology*, 87 (2001) 17–21.
48. Chaubal M.V., Payne G.F., Reynolds C.H., Albright R.L., Equilibria for the adsorption of antibiotics onto neutral polymeric sorbents: experimental and modeling results, *Biotechnology Bioengineering*, 47 (1995) 215–226.
49. Lorphensri O., Intravijit J., Sabatini D.A., Kibbey T.C.G., Osathaphan K., Saiwan C., Sorption of acetaminophen, 17α-ethynyl estradiol, nalidixic acid, and norfloxacin to silica, alumina, and a hydrophobic medium, *Water research*, 40 (2006) 1481–1491.
50. Sithole B.B., Guy R.D., Models for tetracycline in aquatic environments, *Water Air Soil Pollutants*, 32 (1987) 303–321.

51. Atkin R., Craig V.S.J., Wanless E.J., Biggs S., Mechanism of cationic surfactant adsorption at the solid-aqueous interface, *Advances in Colloid and Interface Science*, 103 (2003) 219–304.
52. Slishic N.F., Nosach L.V., Voronina O.E., Adsorption of tetracycline-type antibiotics on the surface of finely divided silica, *Khimiya, Fizika ta Tekhnologiya Poverkhni*, 10 (2004) 170–174.
53. Parolo M.E., Savini M.C., Vallés J.M., Baschini M.T., Avena M.J., Tetracycline adsorption on montmorillonite: pH and ionic strength effects, *Applied Clay Science*, 40 (2008) 179–186.
54. Lehninger A.L., Biochemistry, 2d edition, Worth Publishers, INC, New York, 1976.
55. Tadros T.F., Applied Surfactants. Principles and Applications, Wiley-VCH Verlag GmbH & Co. KGaA, Weinheim, 2005.
56. Means J.C., Influence of salinity upon sediment–water partitioning of aromatic hydrocarbons, *Marine Chemistry*, 51 (1995) 3–16.
57. Zhang Y., Zhou J.L., Removal of estrone and 17β-estradiol from water by adsorption, *Water Research* 39 (2005) 3991–4003.
58. Yoon R.-H., Vivek S., Effect of Shirt-Chain Alcohols and Pyridine on the Hydration Forces between silica Surfaces, *Journal of Colloid and Interface Science*, 204 (1998) 179–187.
59. Poortinga A.T., Bos R., Norde W., Busscher H.J., Electric double layer interactions in bacterial adhesion to surfaces, *Surface Science Reports*, 47 (2002) 1-32.
60. van der Wal A., Norde W., Zehnder A.J.B., Lyklema J., *Colloids and Surfaces. B: Biointerfaces*, 9 (1997) 81–100.
61. Rijanaarts H.H.M., Norde W., Lyklema J., Zehnder A.J.B., *Colloids and Surfaces. B: Biointerfaces*, 4 (1995) 191–197.
62. Matsuda N., Agui W., Ogino K., Kawashima N., Watanabe T., Sakai H., Abe A., Disinfection of viable *Pseudomonas stutzeri* in ultrapure water

with ion exchange resins, *Colloids and Surfaces. B: Biointerfaces*, 7 (1996) 91-100.

63. Sullivan E.J., Carey J.W., Bowman R.S., Thermodynamics of Cationic Surfactant Sorption onto Natural Clinoptilolite, *Journal of Colloid and Interface Science*, 206 (1998) 369–380.
64. Chung J. J., Lee S. W., Kim Y. C., Solubilization of Alcohols in Aqueous Solution of Cetylpyridinium Chloride, *Bull. Korean Chem. Soc*., 13 (1992) 647–649.
65. Mittal K.L., Micellization, Solubilization, and Microemulsions, V. I, Plenum Press New York, 1977.
66. Golub T.P., Koopal L.K., Adsorption of Cationic Surfactants on Silica. Comparison of Experiment and Theory, *Langmuir*, 13 (1997) 673–681.
67. Sineva A.V., Parfenova A.M., Fedorova A.A., Adsorption of micelle forming and non-micelle forming surfactants on the adsorbents of different nature, Colloid *and Surface A: Physiochemical and Engineering Aspects*, 306 (2007) 68–74.
68. Lee E.M., Koopal L.K., Adsorption of Cationic and Anionic Surfactants on Metal Oxide Surface: Surface Charge Adjustment and Competition Effects, *Journal of Colloid and Interface Science*, 177 (1996) 478–489.
69. Manne S., Cleveland J.P., Gaub H.E., Stucky G.D., Hansma P.K., Direct Visualization of Surfactant Hemimicelles by Force Microscopy of the Electrical Double Layer, *Langmuir*, 10 (1994) 4409-4413.
70. Brahimi B., Labbe P., Reverdy G., Study of the Adsorption of Cationic Surfactants on Aqueous Laponite Clay Suspensions and Laponite Clay Modified Electrodes, *Langmuir*, 8 (1992) 1908–1918.
71. Gurses A., Yalcin M., Sozbilir M., Dogan C., The investigation of adsorption thermodynamics and mechanism of a cationic surfactant, CTAB, onto powdered active carbon, *Fuel Processing Technology*, 81 (2003) 57–66.

72. Jandera P., Komers D., Anděl L., Prokeš L., Fitting competitive adsorption isotherms to the distribution data in normal phase systems with binary mobile phase, *Journal of Chromatography*, 831 (1999) 131–148.
73. Warr G.G., Surfactant adsorbed layer structure at solid/solution interfaces: impact and implications of AMF imaging studies, Current *Opinion in Colloid & Interface Science*, 5 (2000) 88–94.
74. Wolgemuth J.L., Workman R.K., Manne S., Surfactant Aggregates at a Flat, Isotropic Hydrophobic Surface, *Langmuir*, 16 (2000) 3077–3081.
75. Tiberg F., Brinck J., Grant L., Adsorption and surface-inducted self-assembly of surfactants at the solid-aqueous interface, *Current Opinion in Colloid & Interface Science*, 4 (2000) 411–419.
76. Harwell J.H., Hoskins J.C., Schechter R.S., Wade W.H., Pseudophase Separation Model for Surfactant Adsorption: Isomerically Pure Surfactants, *Langmuir*, 5 (1985) 1549–1559.
77. Jaschke M., Butt H.-J., Gaub H.E., Manne S., Surfactant Aggregates at a Metal Surface, *Langmuir*, 13 (1997) 1381–1384.
78. Sharma B.G., Basu S., Sharma M.M., Characterization of Adsorbed Ionic Surfactants on a Mica Substrate, *Langmuir*, 12 (1996) 6506–6512.
79. Zhu B.Y., Gu T., General isotherm equation for adsorption of surfactants at solid/liquid interfaces, *Journal of Chemical Society. Faraday Transactions*, 85 (1989) 3813–3817.
80. Böhmer M.R., Koopal L.K., Adsorption of Ionic Surfactants on Constant Charge Surfaces. Analysis Based on a Self-Consistent Field Lattice Model, *Langmuir*, 8 (1992) 1594–1602.
81. van Oss C.J., Hydrophobicity of biosurfaces – origin, quantitative determination and interaction energies, *Colloids and Surfaces B: Biointerfaces*, 5 (1995) 91-110.

APPENDIX I Extended DLVO theory

The relationship between bacteria themselves was investigated in the framework of the extended DLVO theory [81]. According to this theory, bacterial adhesion is in a balance between van der Waals, electrostatic and acid-base interaction forces, and is a function of the separating distance (d):

$$G_{slm}(d) = G_{slm}^{LW}(d) + G_{slm}^{AB}(d) + G_{slm}^{EL}(d) \quad (16)$$

The electrostatic, van der Waals and acid–base interactions between bacterial cells as a function of the ionic strength were calculated by Eqs. (17)–(20) (Table 9), and are displayed in Fig. 20. The total 'interaction energy *vs* separation distance' curves at different ionic strengths are shown in Fig. 21. As seen in Fig. 20, the electrostatic repulsion is higher that the van der Waals attraction at the lowest electrolyte concentration (0.001 M). In addition, the acid-base interaction is very repulsive at close approach. Hence, aggregation of the bacteria is not possible at low ionic strength of the solution.

Table 9. Equations calculating extended DLVO interactions.

Lefshitz-van der Waals interaction energy, $G^{LW}(d)$

Sphere-sphere

$$-\frac{A}{12}\left[\frac{y}{x^2+xy+x}+\frac{y}{x^2+xy+x+y}+2\ln\left(\frac{x^2+xy+x}{x^2+xy+x+y}\right)\right]\left(\frac{1}{1+1.77(2\pi d/\lambda)}\right),\ \lambda=1000\text{Å} \qquad (17)$$

Electrostatic interaction energy, $G^{EL}(d)$

Sphere-sphere $$\frac{\pi\varepsilon_r\varepsilon_0 a_1 a_2\left(\zeta_1^2+\zeta_2^2\right)}{a_1+a_2}\left[\frac{2\zeta_1\zeta_2}{\zeta_1^2+\zeta_2^2}\ln\left(\frac{1+e^{-\kappa d}}{1-e^{-\kappa d}}\right)+\ln\left(1-e^{-\kappa d}\right)\right] \qquad (18)$$

Acid-base interaction energy, $G^{AB}(d)$

Sphere-sphere $$\pi a\lambda\Delta G_0^{AB}e^{\left[(d_0-d)/\lambda\right]} \qquad (20)$$

---

a - sphere radius (bacterial), A – Hamaker constant, d – separation distance

d_0 – minimum separation distance between two surfaces, κ - referred to as the Debye-Hückel parameter or double-layer thickness^{-1}, ε_0, ε_r - permittivity of vacuum and the relative permittivity of water, ζ_m, ζ_s - zeta potentials of the microorganism and resin particles respectively, λ - correlation length of molecules in liquid (≈ 6 Å), x=H/(a_1+a_2), y=a_1/a_2

With the increasing ionic strength, however, the electrostatic repulsion decreases and eventually becomes very small. The Fig. 21 shows that the sum of the interaction energies for 0.01, 0.1, and 0.2 M KCl becomes negative approximately at 7 nm distance separation for 0.01 M KCl and at the 4.5 nm for 0.1, 0.2 M KCl exhibit a secondary minimum. It means that adhesion between the bacteria can be expected. Since the aggregated bacteria have more hydrophilic surface than that of the individual bacteria [62], the adsorption of *B. cereus* onto the hydrophilic Purolite A835 is promoted by

hydrophilic interaction. As a result, the adhesion equilibrium curves in Fig. 9 cross as the ionic strength of the solution increases.

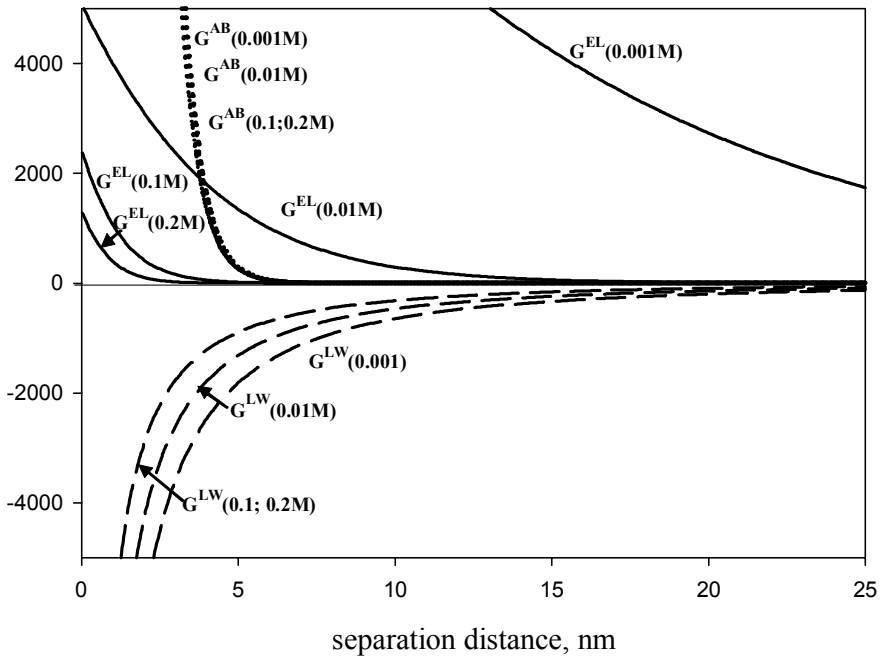

Figure 20. Energy interaction as function separation distance for bacteria-bacteria system.

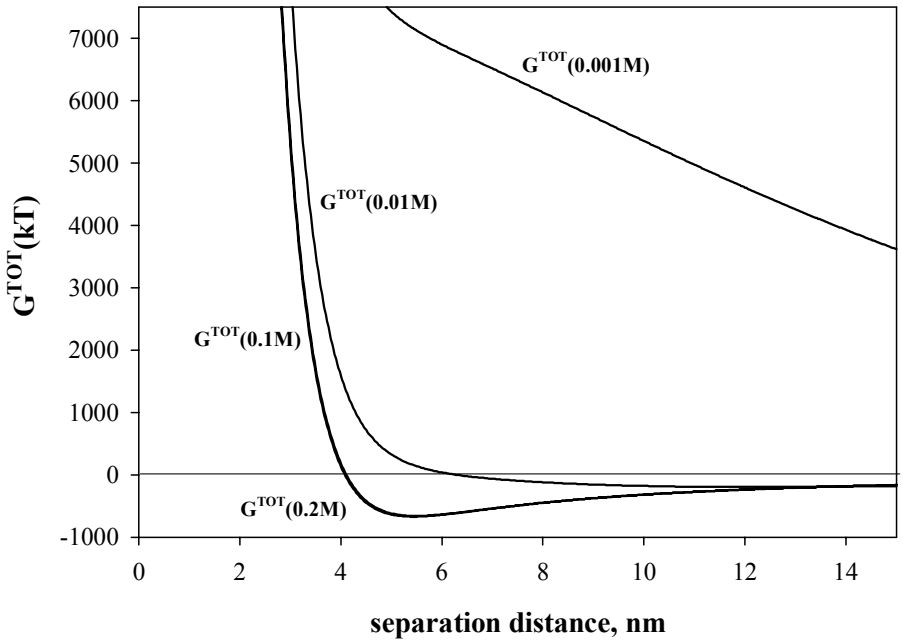

Figure 21. Total interaction energies as a function of separation distance at different ionic strength for bacteria-bacteria system.

ACTA UNIVERSITATIS LAPPEENRANTAENSIS

375. AUVINEN, HARRI. Inversion and assimilation methods with applications in geophysical remote sensing. 2009. Diss.

376. KINDSIGO, MERIT. Wet oxidation of recalcitrant lignin waters: Experimental and kinetic studies. 2009. Diss.

377. PESSI, PEKKA. Novel robot solutions for carrying out field joint welding and machining in the assembly of the vacuum vessel of ITER. 2009. Diss.

378. STRÖM, JUHA-PEKKA. Active d*u*/d*t* filtering for variable-speed AC drives. 2009. Diss.

379. NURMI, SIMO A. Computational and experimental investigation of the grooved roll in paper machine environment. 2009. Diss.

380. HÄKKINEN, ANTTI. The influence of crystallization conditions on the filtration characteristics of sulphathiazole suspensions. 2009. Diss.

381. SYRJÄ, PASI. Pienten osakeyhtiöiden verosuunnittelu – empiirinen tutkimus. 2010. Diss.

382. KERKKÄNEN, ANNASTIINA. Improving demand forecasting practices in the industrial context. 2010. Diss.

383. TAHVANAINEN, KAISA. Managing regulatory risks when outsourcing network-related services in the electricity distribution sector. 2010. Diss.

384. RITALA, PAAVO. Coopetitive advantage – How firms create and appropriate value by collaborating with their competitors. 2010. Diss.

385. RAUVANTO, IRINA. The intrinsic mechanisms of softwood fiber damage in brown stock fiber line unit operations. 2010. Diss.

386. NAUMANEN, VILLE. Multilevel converter modulation: implementation and analysis. 2010. Diss.

387. IKÄVALKO, MARKKU. Contextuality in SME ownership – Studies on owner-managers´ ownership behavior. 2010. Diss.

388. SALOJÄRVI, HANNA. Customer knowledge processing in key account management. 2010. Diss.

389. ITKONEN, TONI. Parallel-operating three-phase voltage source inverters – Circulating current modeling, analysis and mitigation. 2010. Diss.

390. EEROLA, TUOMAS. Computational visual quality of digitally printed images. 2010. Diss.

391. TIAINEN, RISTO. Utilization of a time domain simulator in the technical and economic analysis of a wind turbine electric drive train. 2010. Diss.

392. GRÖNMAN AKI. Numerical modelling of small supersonic axial flow turbines. 2010. Diss.

393. KÄHKÖNEN, ANNI-KAISA. The role of power relations in strategic supply management – A value net approach. 2010. Diss.

394. VIROLAINEN, ILKKA. Johdon coaching: Rajanvetoja, taustateorioita ja prosesseja. 2010. Diss.

395. HONG, JIANZHONG. Cultural aspects of university-industry knowledge interaction. 2010. Diss.

396. AARNIOVUORI, LASSI. Induction motor drive energy efficiency – Simulation and analysis. 2010. Diss.

397. SALMINEN, KRISTIAN. The effects of some furnish and paper structure related factors on wet web tensile and relaxation characteristics. 2010. Diss.

398. WANDERA, CATHERINE. Performance of high power fiber laser cutting of thick-section steel and medium-section aluminium. 2010. Diss.

399. ALATALO, HANNU. Supersaturation-controlled crystallization. 2010. Diss.

400. RUNGI, MAIT. Management of interdependency in project portfolio management. 2010. Diss.

401. PITKÄNEN, HEIKKI. First principles modeling of metallic alloys and alloy surfaces. 2010. Diss.

402. VAHTERISTO, KARI. Kinetic modeling of mechanisms of industrially important organic reactions in gas and liquid phase. 2010. Diss.

403. LAAKKONEN, TOMMI. Distributed control architecture of power electronics building-block-based frequency converters. 2010. Diss.

404. PELTONIEMI, PASI. Phase voltage control and filtering in a converter-fed single-phase customer-end system of the LVDC distribution network. 2010. Diss.

405. TANSKANEN, ANNA. Analysis of electricity distribution network operation business models and capitalization of control room functions with DMS. 2010. Diss.

406. PIIRAINEN, KALLE A. IDEAS for strategic technology management: Design of an electronically mediated scenario process. 2010. Diss.

407. JOKINEN, MARKKU. Centralized motion control of a linear tooth belt drive: Analysis of the performance and limitations. 2010. Diss.

408. KÄMÄRI, VESA. Kumppanuusohjelman strateginen johtaminen – Monitapaustutkimus puolustushallinnossa. 2010. Diss.

409. KARJALAINEN, AHTI. Online ultrasound measurements of membrane compaction. 2010. Diss.

410. LOHTANDER, MIKA. On the development of object functions and restrictions for shapes made with a turret punch press. 2010. Diss.

411. SIHVO, VILLE. Insulated system in an integrated motor compressor. 2010. Diss.

412. SADOVNIKOV, ALBERT. Computational evaluation of print unevenness according to human vision. 2010. Diss.

413. SJÖGREN, HELENA. Osingonjakopäätökset pienissä osakeyhtiöissä. Empiirinen tutkimus osakeyhtiölain varojenjakosäännösten toteutumisesta. 2010. Diss.

414. KAUPPI, TOMI. Eye fundus image analysis for automatic detection of diabetic retinopathy. 2010. Diss.

415. ZAKHVALINSKII, VASILII. Magnetic and transport properties of $LaMnO_{3+\delta}$, $La_{1-x}Ca_xMnO_3$, $La_{1-x}Ca_xMn_{1-y}Fe_yO_3$ and $La_{1-x}Sr_xMn_{1-y}Fe_yO_3$. 2010. Diss.

416. HATAKKA, HENRY. Effect of hydrodynamics on modelling, monitoring and control of crystallization. 2010. Diss.

417. SAMPO, JOUNI. On convergence of transforms based on parabolic scaling. 2010. Diss.